

**NASA
Reference
Publication
1278**

1992

A Self-Zeroing Capacitance Probe for Water Wave Measurements

Steven R. Long
*Wallops Flight Facility
Wallops Island, Virginia*



National Aeronautics and
Space Administration
Office of Management
Scientific and Technical
Information Program





TABLE OF CONTENTS

1.0 INTRODUCTION	1
2.0 CIRCUIT DESIGN AND CONSTRUCTION	2
2.1 Background and Development	2
2.2 Circuit Principles and Design	3
2.3 The Detailed Circuit	5
2.4 Circuit Board Layout and Wiring Diagrams	6
3.0 WIRE PROBE CONSTRUCTION	7
4.0 LIMITATIONS	8
5.0 CALIBRATION	9
6.0 SUMMARY	9
7.0 ACKNOWLEDGEMENTS	10
8.0 REFERENCES	10
9.0 APPENDIX	12

FIGURE CAPTIONS

- Fig. 2.1 The fundamental block diagram of the circuit
- Fig. 2.2 The detailed circuit diagram
- Fig. 2.3 The frequency characteristic curve of the 60 Hz notch filter
- Fig. 2.4 The circuit card, socket-side view
- Fig. 2.5 The circuit card, pin-side view
- Fig. 2.6 to Fig. 2.26 Wiring diagrams giving interconnections
- Fig. 2.27 Plug-in tab connections
- Fig. 3.1 Laboratory arrangement of the wire probe
- Fig. 3.2 The triax connection
- Fig. 5.1 Typical results of probe calibration

1.0 INTRODUCTION

The wave probe developed at the Air-Sea Interaction Research Facility was designed to measure the surface elevation fluctuations of water waves. Design criteria included being linear in response, self-zeroing to the mean water level, having multiple operating ranges so that the instrument's maximum output could be matched to the maximum surface elevation over varying conditions, and be as noise-free as possible.

Historically, research efforts utilizing the measurement of wave surface elevations at sea or in the laboratory have been divided along two main approaches: using a resistive change or a capacitive change which is induced by a change in water level, and thus a measure of surface elevation. Representative of the resistive-type of instrument is that described by the National Oceanographic Instrumentation Center (1974), and that used by Mitsuyasu and Honda (1974). Capacitive-type instruments have been discussed by McGoldrick (1965, 1969, 1971) and Mitsuyasu (1968), among others.

The wave probe described here is of the capacitive-type, incorporating several features as mentioned above which were previously unavailable. These added design criteria both increase the ease of operation and the reliability of the results.

2.0 CIRCUIT DESIGN AND CONSTRUCTION

2.1 Background and Development

Any insulated conductor may be used as a probe. The principle of the probe is to use the insulated conductor and the tank as the two plates of a capacitor. Any change in the water level would change the dielectric effect between the plates, which is then measured via impedance balancing.

A basic characteristic of the capacitive-type probes used previously has been impedance balancing via an adjustable impedance bridge or tunable tank circuit within the probe circuit. The circuit would then be configured for a data run and then adjusted in the quiescent (zero signal) condition to effect a zero output voltage by balancing the impedance (capacitance) of the probe apparatus. The mechanism by which zeroing was accomplished was basically a subtraction or cancellation of the impedance (capacitance) of the entire probe assembly. For small wave heights, the capacitance changes that occur because of wave action may be quite possibly only 10^{-3} of the total probe apparatus capacitance. The frustrations that can result in attempting to maintain a satisfactory zero calibration or to compensate for the lack of it in such circumstances is obvious.

The capacitance probe that is the subject here avoids this problem by "bootstrapping" a guard circuit (shield) to the probe sense line. In effect, the capacitance that exists in a shielded cable between the center conductor and the shield is in this circuit reduced by a factor approaching 10^5 .

This is accomplished by driving the shield of the probe sense line to eliminate (10^{-5}) the voltage potential that would otherwise exist across the intervening dielectric. A second outer shield is grounded to effect normal system shielding. Thus triax cable (Triaxial, double shielded) and connectors are used between the circuit and the wire probe used for the elevation measurements.

In many previously used probe systems, variations in the capacitance of the probe coupling apparatus (cable, etc.) was transferred to the output data. For small signal levels, this could have been a significant source of error, either directly or through measurement equipment nonlinearities. In the probe presented here, the effective capacitance of the probe coupling apparatus is reduced to a negligible value. Thus this probe achieves automatic self-zeroing to the mean water level with a time constant easily adjustable, effectively canceling the cable length effects, cable flexing effects, etc., and providing long term stability during measurements.

2.2 Circuit Principles and Design

The fundamental block diagram of the circuit is shown in Figure 2.1. An oscillator is used to generate a 20 KHz sine wave, which is directed through two different branches of the circuit. The first branch leads through the pulse forming network (I) to a latch circuit. The second branch leads to a negative feedback (NFB) amplifier. It is here that cable effects are canceled, and the water waves introduce their surface elevation information by varying the capacitance C_x . The larger C_x becomes, the smaller the gain becomes of the NFB amplifier. The path then leads on to the pulse forming network (II) to the latch circuit.

The function of the pulse forming network is to transform the sine waves into square waves whose pulse width is determined by the amplitude of the sine waves. Thus in the second branch, the water waves cause the pulse width to vary with changes in water surface elevation. Within the first branch, no such variation is caused in the pulse width.

Both pulse forming branches lead to the latch circuit. Here the pulse widths of the signals from the two pulse forming networks are compared. The pulse duration of the output of the latch depends on the difference of the two pulse widths compared. When the value of the C_x capacitance increases, the latch pulse output width increases also. Receiving the latch output, a filter network transforms it into a DC signal which is then passed to a DC amplifier. It is here that the various range selections are implemented, by adjusting the gain of the DC amplifier. In order to reduce the effects of 60 Hz noise, the signal is passed through a 60 Hz notch filter, and finally through another DC amplifier network to produce the final output signal.

Because the performance of components is not totally uniform (5% tolerance on resistors, for example), the output levels of different wave probes of the identical circuit design will be slightly different, even for identical water surface changes. This is compensated at the time of calibration, so that each probe circuit board will have its own set of calibration constants.

2.3 The Detailed Circuit

The complete circuit is shown in Figure 2.2, and was arranged to fit on a standard plug-in type circuit card. An integrated circuit, labeled PB13, of the type MC1458CP, is used in the 20 KHz oscillator. The amplitude of the sine waves produced is 10 v peak-to-peak. PB16, which is half of an MC1458CP, serves as the NFB amplifier. The two pulse forming networks from Figure 2.1 are formed within PB14 (LM339N) and PB15 (7400N). The latch network receiving the two pulse forming branches (see Figure 2.1) in Figure 2.2 is labeled PB11, of the type 74279. The filter to transform the latch output into a DC level is at PB10, consisting of the 22 K Ω resistors and one 0.047 μ f capacitor. DC amplification occurs in three stages at PB09 (half of MC1458CP), PB08 (half of MC1458CP), and PB06 (CA3140). The gain adjustment occurs at one stage of the three stage DC amplification, at PB09, where gain is adjusted by selecting a resistor by switch selection. The resistor selected becomes part of the negative feedback, and is located on PB19.

PB01 (half of MC1458CP) and twin filters on PB02 constitute the 60 Hz notch filter. The notching frequency is dependent on the value of the resistor and capacitor on the input side of the twin filters, and is given by

$$f = \frac{1}{2\pi RC}$$

where f is the frequency dominated by the notch, R is the resistor value in ohms, and C is the capacitor value in farads. The frequency characteristic curve of a typical notch filter measurement

is shown as Figure 2.3. Using the notch filter suppresses the 60 Hz noise by at least 15 dB. The final output emerges from PB01 (half of MC 1458CP), and PB21 (CA3140), which form the output DC amplifier. The wave forms at each stage for testing purposes are illustrated in Table 2.1.

2.4 Circuit Board Layout and Wiring Diagrams

The circuit components were installed on a standard IC circuit card (Vector 3682-4), using standard IC sockets, and wire-wrapping techniques for interconnections. The components were installed on 21 IC sockets, arranged as shown in Figures 2.4 and 2.5, giving the socket and pin-side view respectively. A numbering code is used to give both the socket location and pin number for the connections in each of the wiring diagrams, Figures 2.6 to 2.26. As an example, consider the wiring diagram of Figure 2.6 on the pin side of the illustration, where pin 7 is shown to connect to "0316." This is an instruction to connect this pin to PB03 on pin 16. Pin 1 is seen to connect to pin 2, while pin 2 is connected to "0213," which is PB02 and pin 13. This numbering code is used throughout the wiring diagrams. The circuit card itself is PB00.

In addition to the connections between sockets, connections are also needed between the sockets and the IC circuit card plug-in tabs. These are given in Figure 2.27, where the circuit card itself is considered to be PB00. A complete listing of components is given in the Appendix.

3.0 WIRE PROBE CONSTRUCTION

Any well insulated conductor may be used as a probe. The characteristics of the insulation, such as dielectric constant, thickness, etc., will effect the response per unit length. Thus wire selection will be influenced by the wave conditions expected, and a separate calibration would be needed for each wire type.

For our laboratory application, we chose a #30 AWG solid copper wire manufactured by Belden as "heavy armored polythermaleze." The usual use for this wire is to wrap electric motors, make inductors, etc. Sizes down to #44 were also tried, but no measurable increase in frequency response was noted. With such a small size as #44, the probes proved to be too fragile, so that a #30 AWG was finally selected for our application.

To effect a negligible conductance, the submerged (unprotected) end of the cut wire must be sealed against water. In our application, a monofilament fishing line was joined to the wire at the submerged end to provide the necessary tension in the probe when placed under constant tension from a standard rubber band. Additionally, it must be noted that a uniform wire depth of immersion is important to maintain the resulting calibration and the desired interchangeability of wires, since the circuit here described responds to

$$\frac{\Delta C}{C} ,$$

where C is the capacitance, and ΔC is the change in capacitance caused by the wave motion. This

arrangement is shown in Figure 3.1.

The joint between monofilament and wire was first made by a knot which was then covered with standard epoxy, followed by a red heat shrink tube (T & B type). Once shrunk, the extra wet epoxy was ejected from the ends of the heat shrink tube, and used to coat the entire tube exterior with epoxy. After proper curing, the final coat was a thin film of silicon rubber (RTV). The probe wire was then attached to a triax connector, as shown in Figure 3.2, with care being taken to insure a uniform immersion depth and a good electrical connection at the triax connector (remove enough wire coating to connect electrically). The immersion depth used in our laboratory application is 15 cm. Once mounted to the triax connector, the probes can be easily removed or replaced.

4.0 LIMITATIONS

An important limiting factor for wire probes measuring the surface elevation of water waves is the frequency limiting effects of the meniscus. Its diameter defines a spot size for the measurements. As the wave lengths approach this spot size diameter, the probe can no longer accurately measure the waves. As shown by Sturm and Sorrell (1973) and discussed by Long and Huang (1976), a practical limit of approximately 12 to 15 Hz exists for even the smallest of probe diameters, due to the meniscus. Thus, even though the circuit itself can accurately measure capacitance changes at frequencies far beyond this, the water waves are unable to cause such high frequency capacitance variations due to the presence of the meniscus. Additionally, frequencies

under 0.1 Hz can not be accurately followed due to the circuit's self-zeroing feature, without first changing the time delay value in the circuit.

5.0 CALIBRATION

Numerous concepts may be considered for calibration of surface elevation probes. The selection should depend upon the physical system and available facilities in which the probes will be employed. One method which has been used at our facility is to group several probes together within a radius of a centimeter or two, and use smooth sine waves of low frequency (about 1.5 Hz) generated by the hydraulic wave generator. The amplitude was accurately measured at the probe location, and the output voltage was digitized by computer interfaced equipment. This was repeated for a variety of wave amplitudes, and the output voltages noted for the various ranges. This produced results that are presented graphically in Figure 5.1.

6.0 SUMMARY

The wave probe developed at the Air-Sea Interaction Research Facility has met the design criteria of being linear in response, self-zeroing to the mean water level, having multiple operating ranges for maximum resolution, and being as noise free and accurate as possible. It is a reliable probe that is well suited to laboratory conditions, with the added flexibility of being adaptable for field work with the proper choice of coated probe wire and calibration resistors.

7.0 ACKNOWLEDGEMENTS

The author wishes to acknowledge the key contributions of Robert Snyder, now retired from NASA GSFC / WFF, who designed and tested the wave probe circuits, Dr. Quanan Zheng of the University of Delaware, who worked out the wire wrap interconnection diagrams, and built the wire wrapped circuit board set described in this document, and Dr. Norden E. Huang, for his invaluable discussions and suggestions.

8.0 REFERENCES

Long, S. R., and N. E. Huang (1976). On the variation and growth of wave-slope spectra in the capillary-gravity range with increasing wind, J. Fluid Mech., 77, 209-228.

McGoldrick, L. F. (1965). Report No. 1, Wave Measurement Systems. The Johns Hopkins Gravitohydrodynamics Laboratory, September 1965.

McGoldrick, L. F. (1969). Technical Report No. 3, Contract N00014-67-A-0285-0002, Office of Naval Research, August 1969.

McGoldrick, L. F. (1971). A sensitive linear capacitance-to-voltage converter, with applications to surface wave measurements, Rev. Sci. Inst., 42, 359-361.

Mitsuyasu, H. (1968). On the growth of the spectrum of wind-generated waves (I), Rep. Res. Inst. Appl. Mech., Kyushu Univ., 16, No. 55, 459-482.

Mitsuyasu, H. and T. Honda (1974). The high frequency spectrum of wind-generated waves, J. Ocean. Soc. Japan, 30, 185-198.

National Oceanographic Instrumentation Center (1974). Instrument Fact Sheet, IFS-74009, NOAA, May 1974.










Sturm, G. V. and F. Y. Sorrell (1973). Optical wave measurement technique and experimental comparison with wave height probes, Appl. Opt., 12, 1928-1933.

APPENDIX

LIST OF COMPONENTS

<u>Description</u>	<u>Quantity</u>
Integrated Circuit	
CM1458CP	5
CA3140	2
74219N	1
7400N	1
LM339N	1
Resistor	
100 Ω , 1/4W, 5%	2
330 Ω , 1/4W, 5%	2
1.5 K Ω , 1/4W, 5%	1
1.8 K Ω , 1/4W, 5%	1
2.7 K Ω , 1/4W, 5%	1
3.9 K Ω , 1/4W, 5%	3
4.7 K Ω , 1/4W, 5%	3
5.6 K Ω , 1/4W, 5%	6
8.2 K Ω , 1/4W, 5%	1
10 K Ω , 1/4W, 5%	1
12 K Ω , 1/4W, 5%	1
22 K Ω , 1/4W, 5%	4
39 K Ω , 1/4W, 5%	1
47 K Ω , 1/4W, 5%	1
68 K Ω , 1/4W, 5%	2
82 K Ω , 1/4W, 5%	2
100 K Ω , 1/4W, 5%	3
120 K Ω , 1/4W, 5%	1
220 K Ω , 1/4W, 5%	1
270 K Ω , 1/4W, 5%	2
390 K Ω , 1/4W, 5%	2
1 M Ω , 1/4W, 5%	1
6.8 M Ω , 1/4W, 5%	1
Capacitor	
0.001 μ f 50V 5%	2
0.0027 μ f 50V 5%	3
0.01 μ f 50V 5%	3
0.022 μ f 50V 5%	1
0.033 μ f 50V 5%	5
0.047 μ f 50V 5%	2
0.068 μ f 50V 5%	2
3.3 μ f 35V 10%	2
4.7 μ f 35V 10%	3

Table 1. Wave Forms of Each Stage.

Part Location	Pin Number	Wiring Code	Wave Form	Description
PB13	07	1307		20 KHz Sine Wave, 10V P-P
PB16	01	1601		20 KHz Sine Wave, 10V P-P
PB14	02	1402		20 KHz Square Wave, 16V
PB14	13	1413		20 KHz Square Wave, 16V
PB15	03	1503		20 KHz Square Wave, 3.8V
PB15	11	1511		20 KHz Square Wave, 3.8V
PB15	06	1506		20 KHz Negative Pulse, 4.2V
PB15	08	1508		20 KHz Negative Pulse, 4.2V
PB11	07	1107		20 KHz Positive Pulse, 3.8V
PB09	01	0901		DC, -2V
PB08	01	0801		DC, -2V
PB06	06	0606		DC, 0 V
PB09	07	0907		DC, 0 V
PB01	01	0101		DC, 0 V
PB01	07	0107		DC, 0 V
PB21	06	2106		DC, 0 V

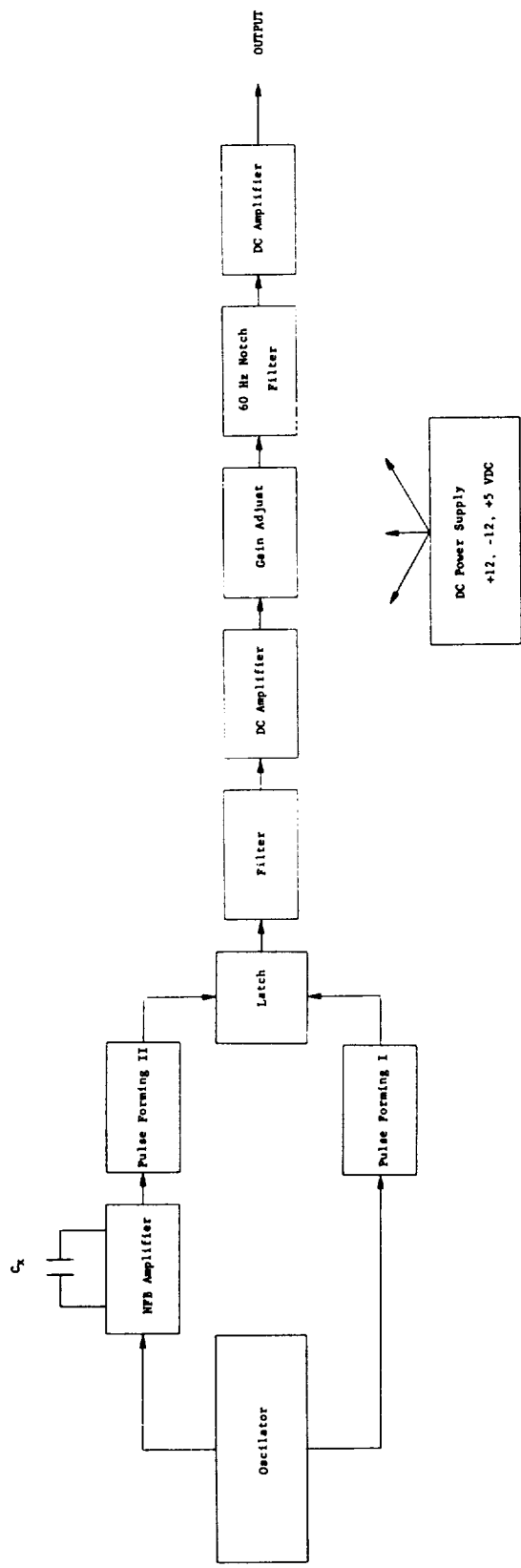


Figure 2.1. The fundamental block diagram of the circuit.

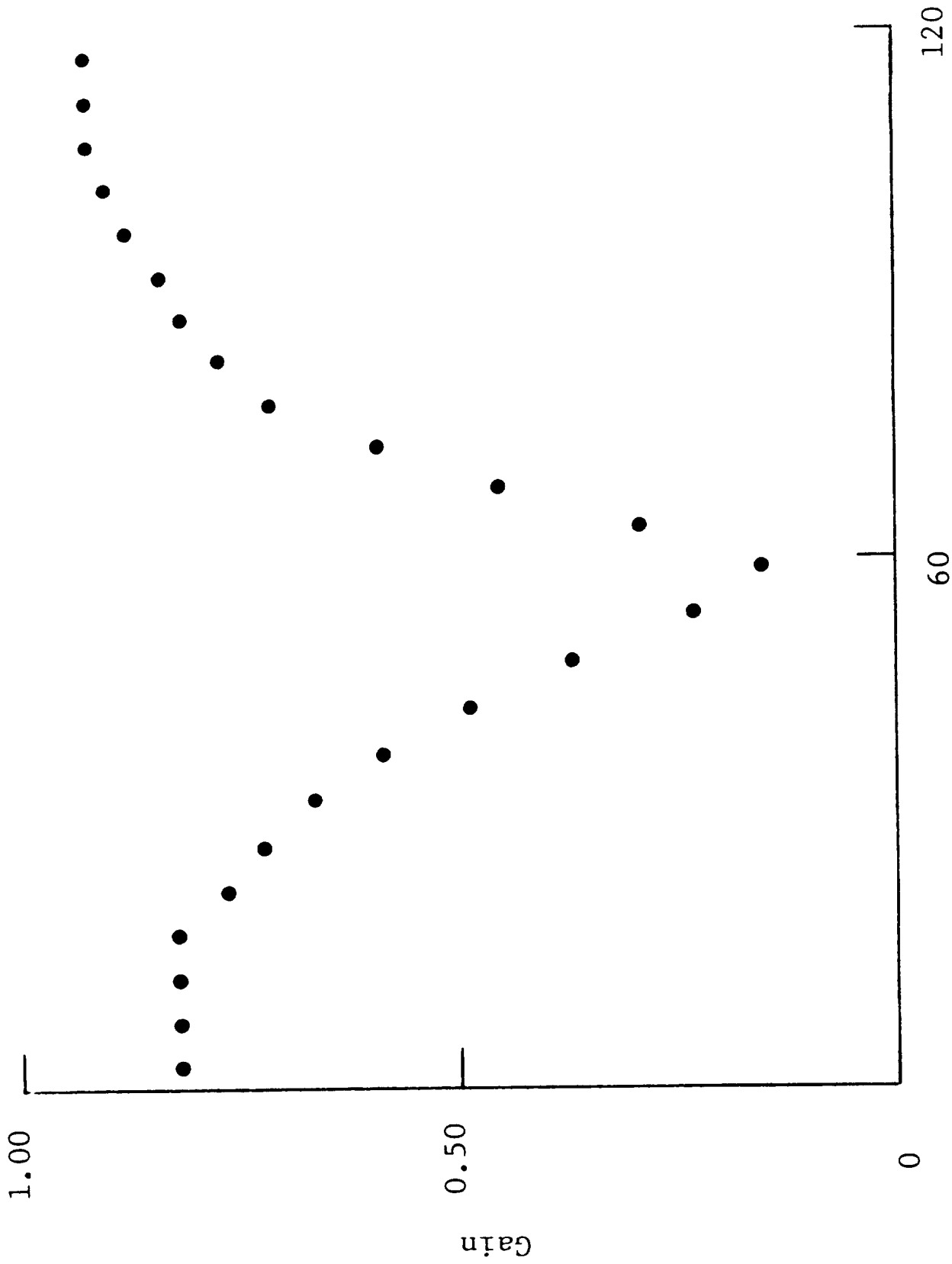


Figure 2.3. The frequency characteristic curve of the 60-Hz notch filter.

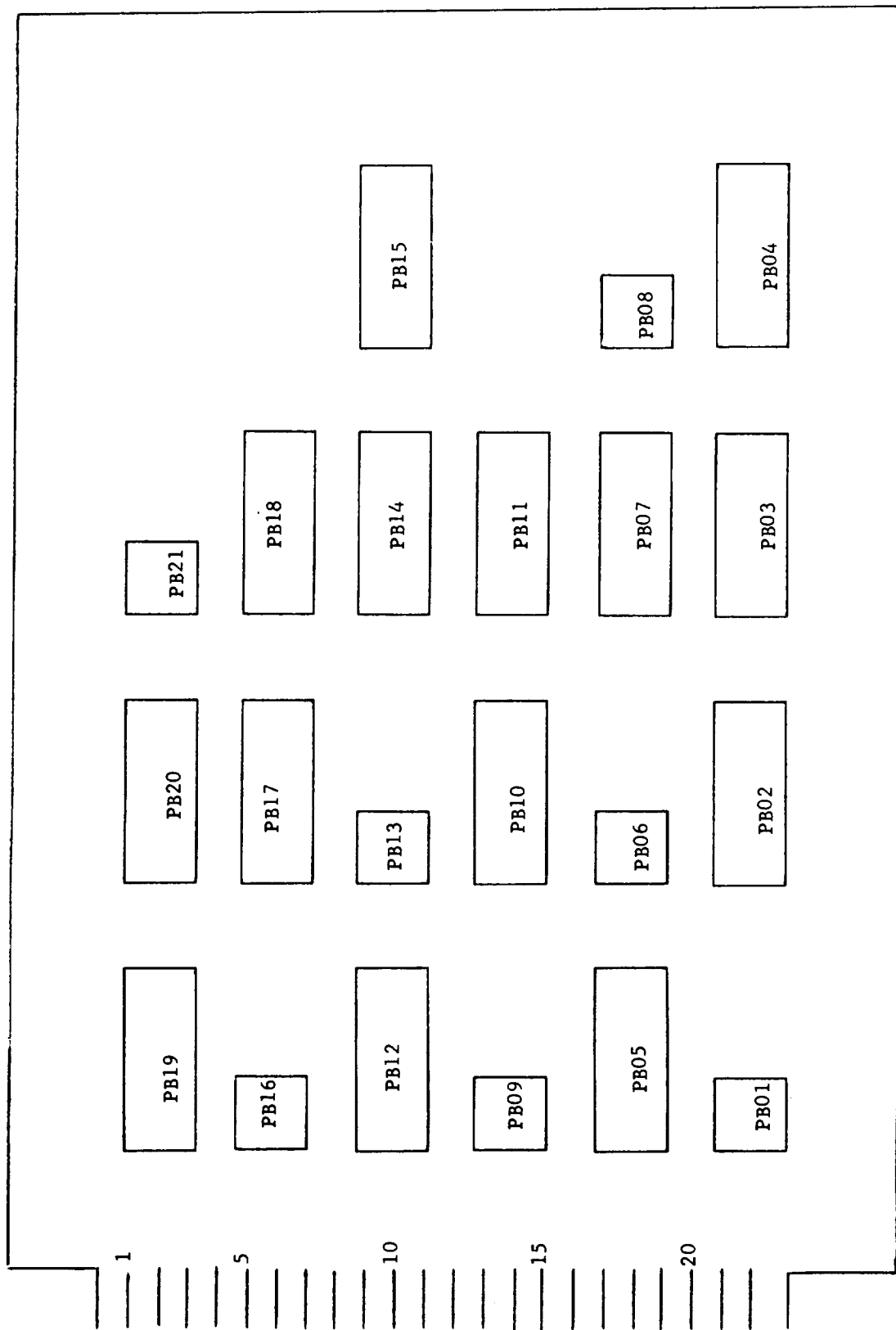


Figure 2.4. The circuit card, socket-side view.

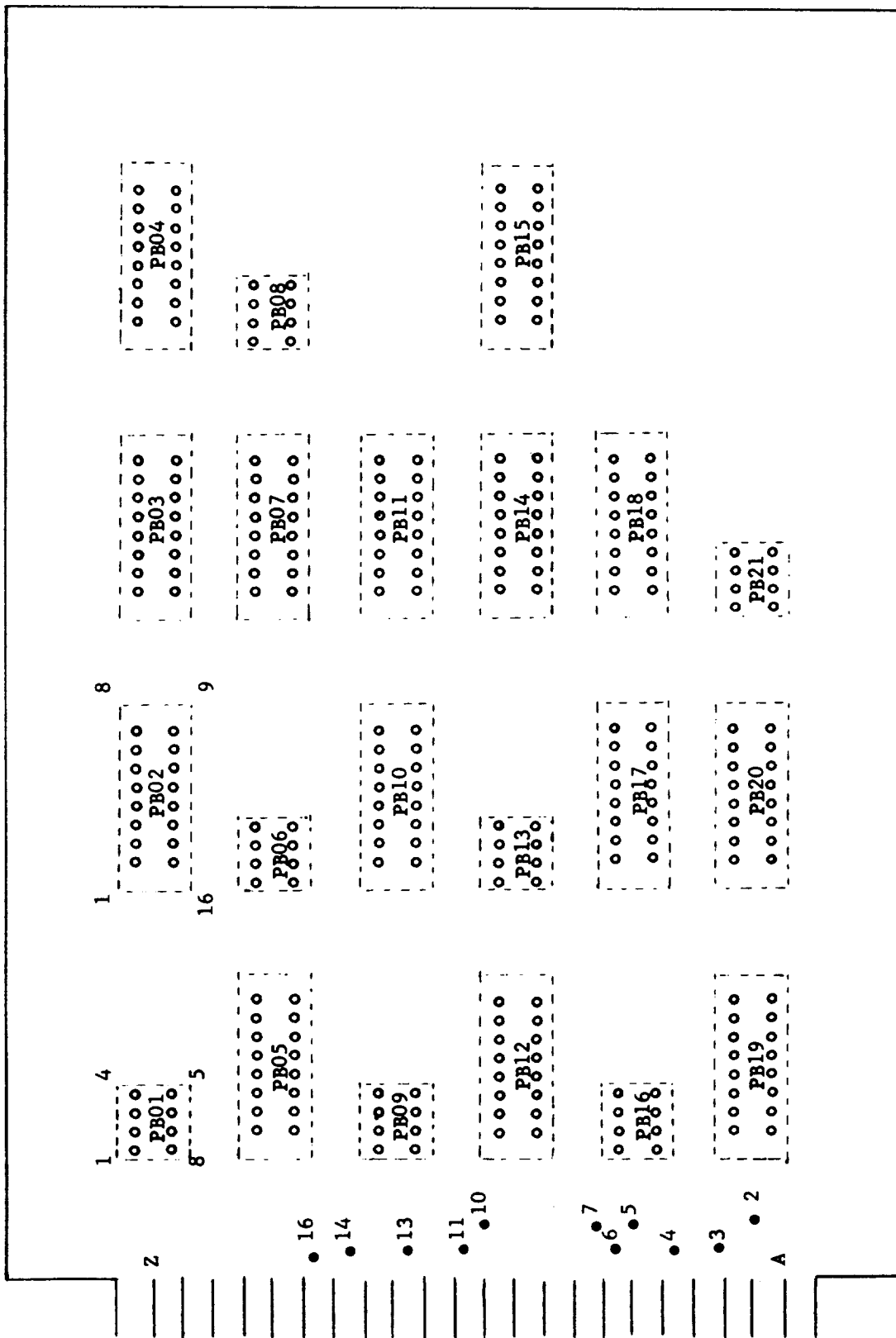
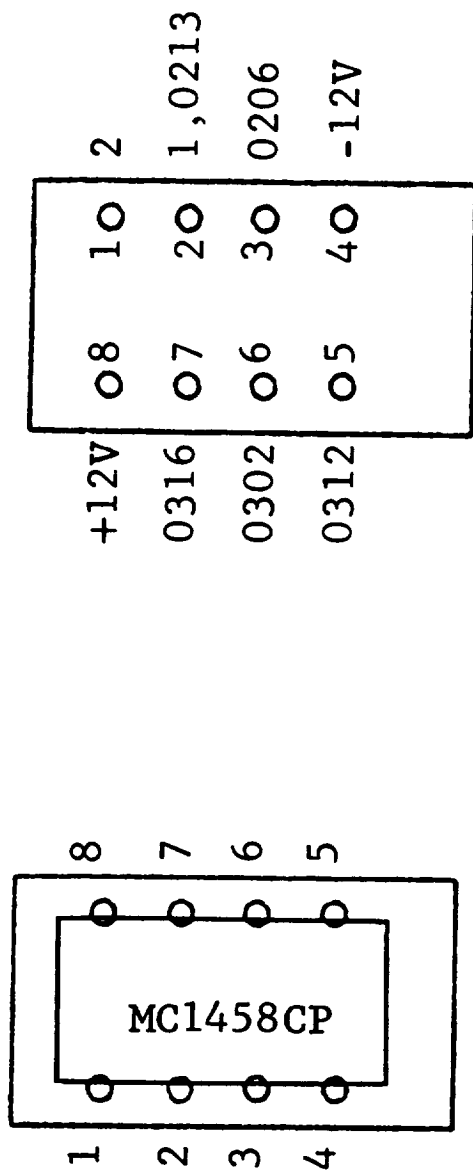
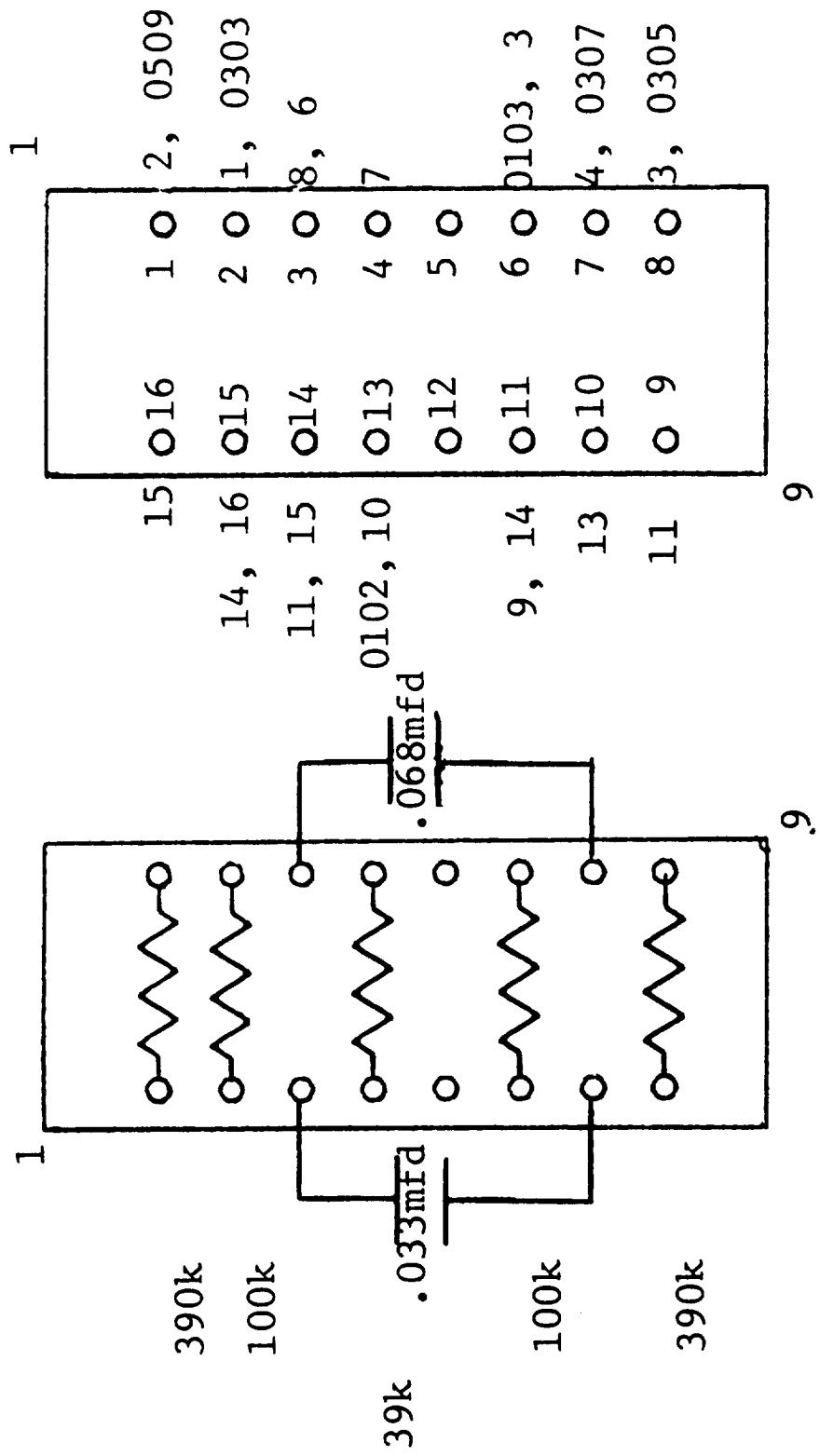


Figure 2.5. The circuit card, pin-side view.



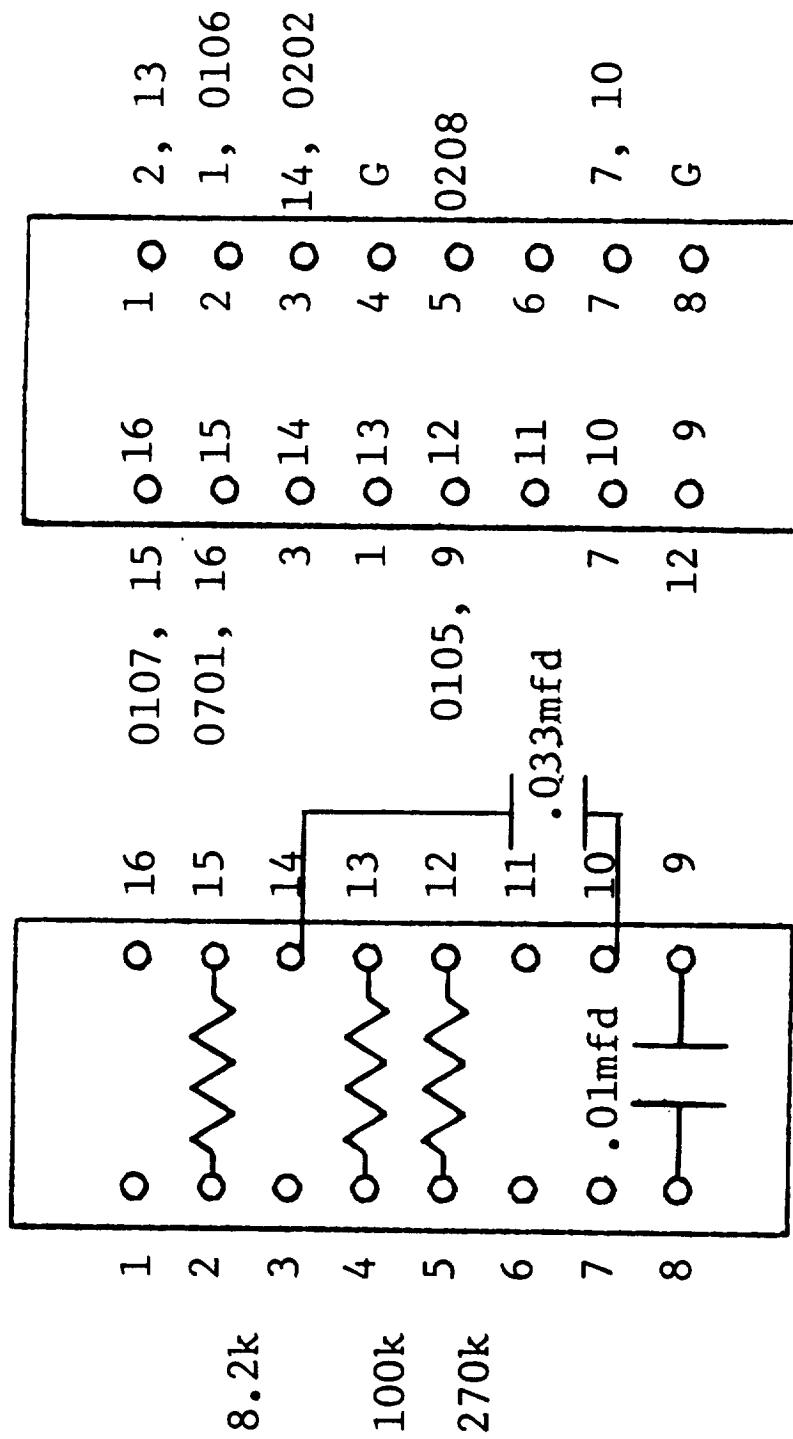
PB01

Figure 2.6. Wiring diagram with interconnections.



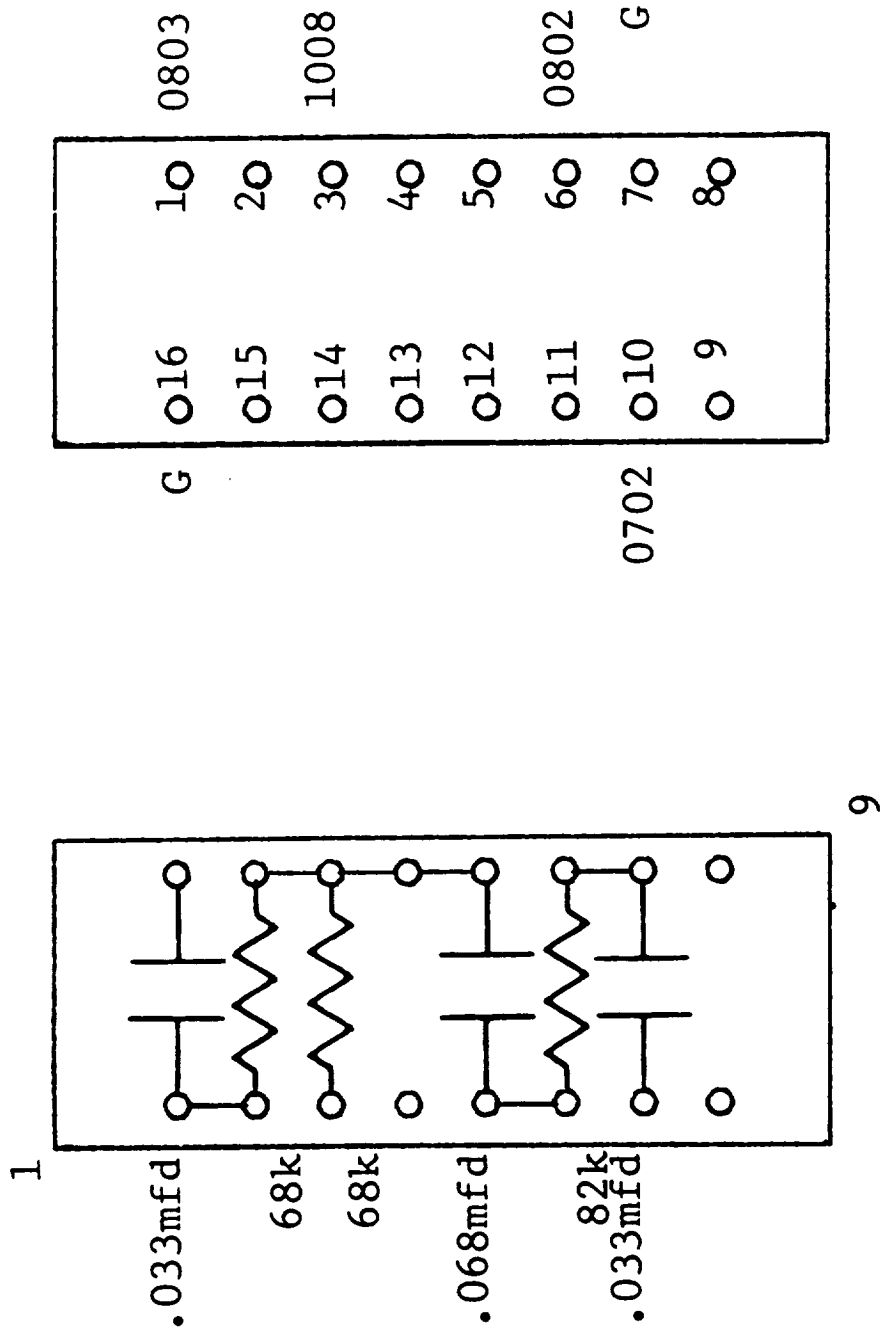
PB02

Figure 2.7. Wiring diagram with interconnections.



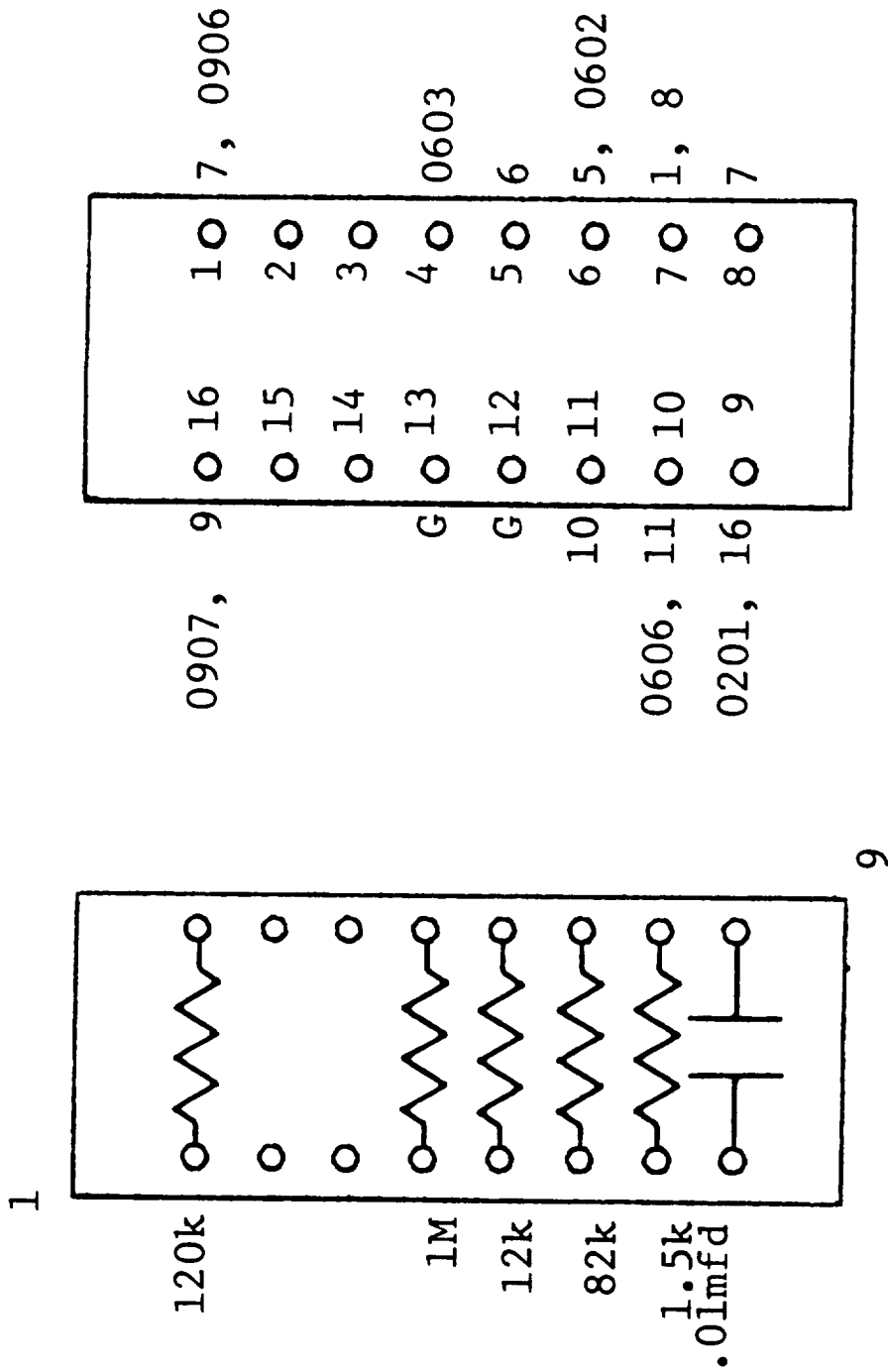
PB03

Figure 2.8. Wiring diagram with interconnections.



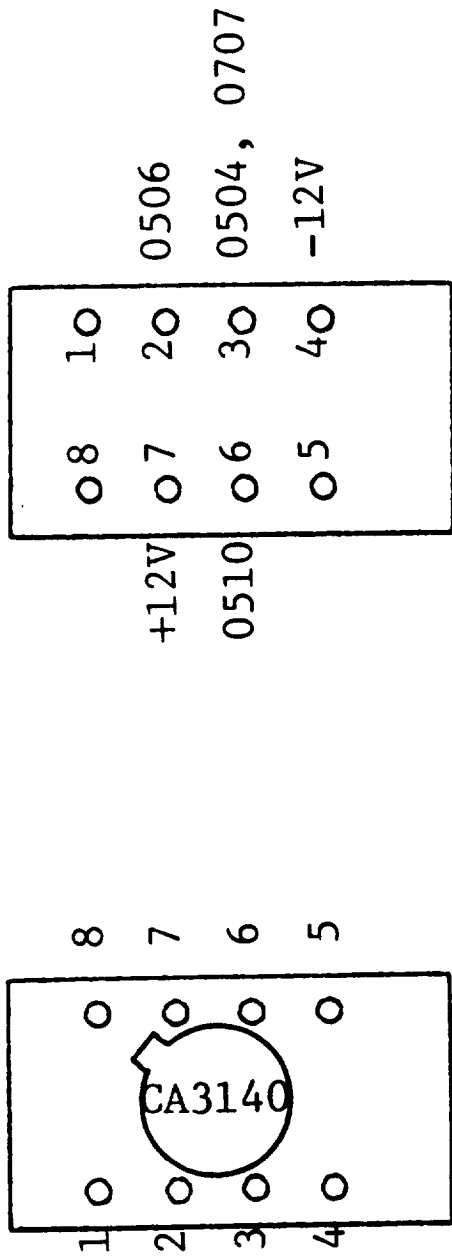
PB04

Figure 2.9. Wiring diagram with interconnections.



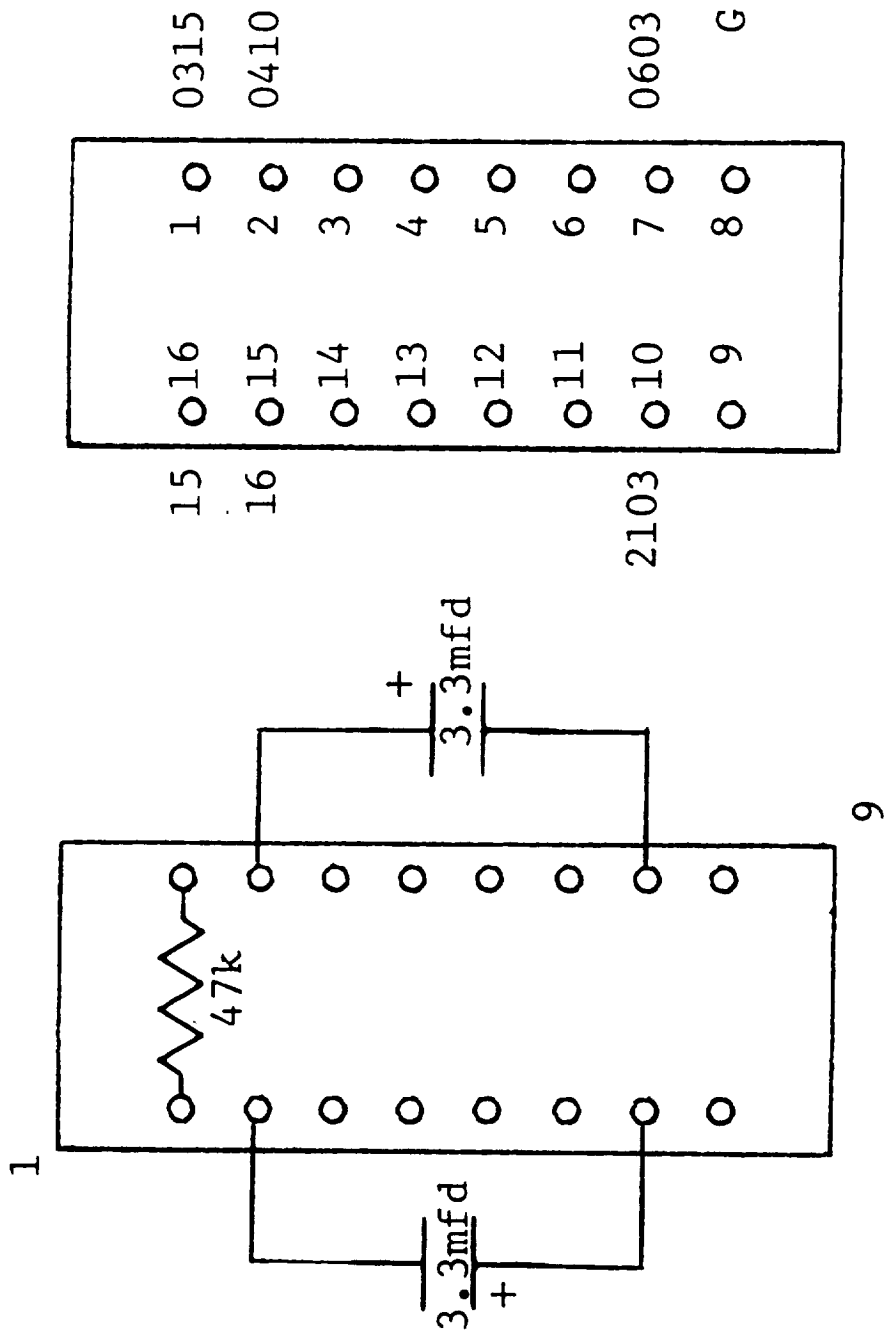
PB05

Figure 2.10. Wiring diagram with interconnections.



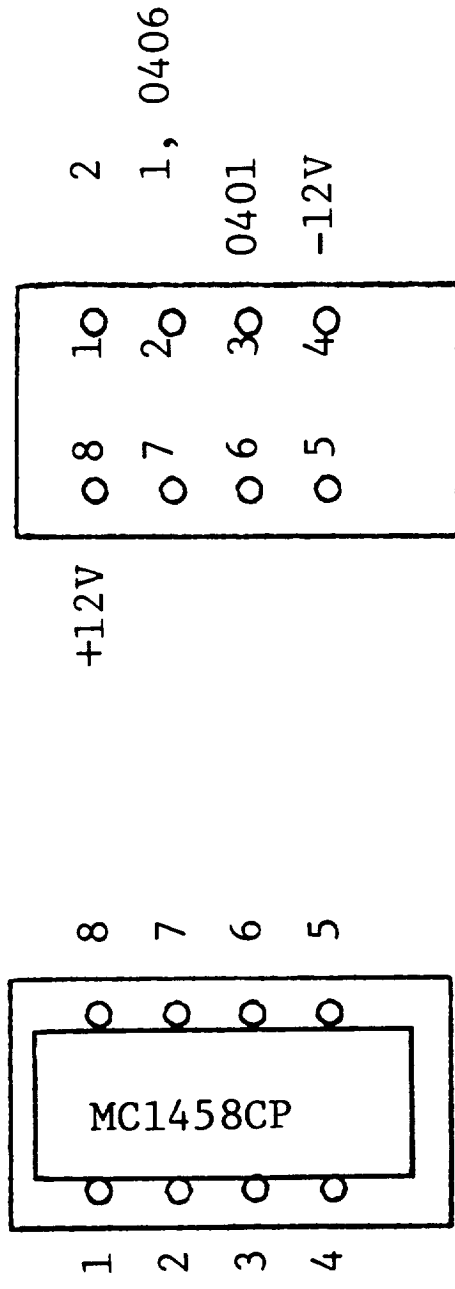
PB06

Figure 2.11. Wiring diagram with interconnections.



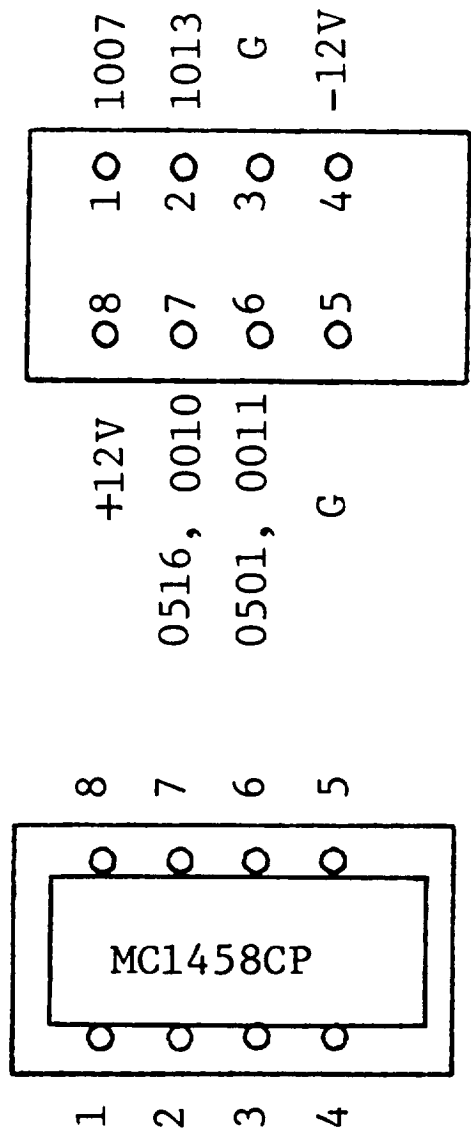
PB07

Figure 2.12. Wiring diagram with interconnections.



PB08

Figure 2.13. Wiring diagram with interconnections.



PB09

Figure 2.14. Wiring diagram with interconnections.

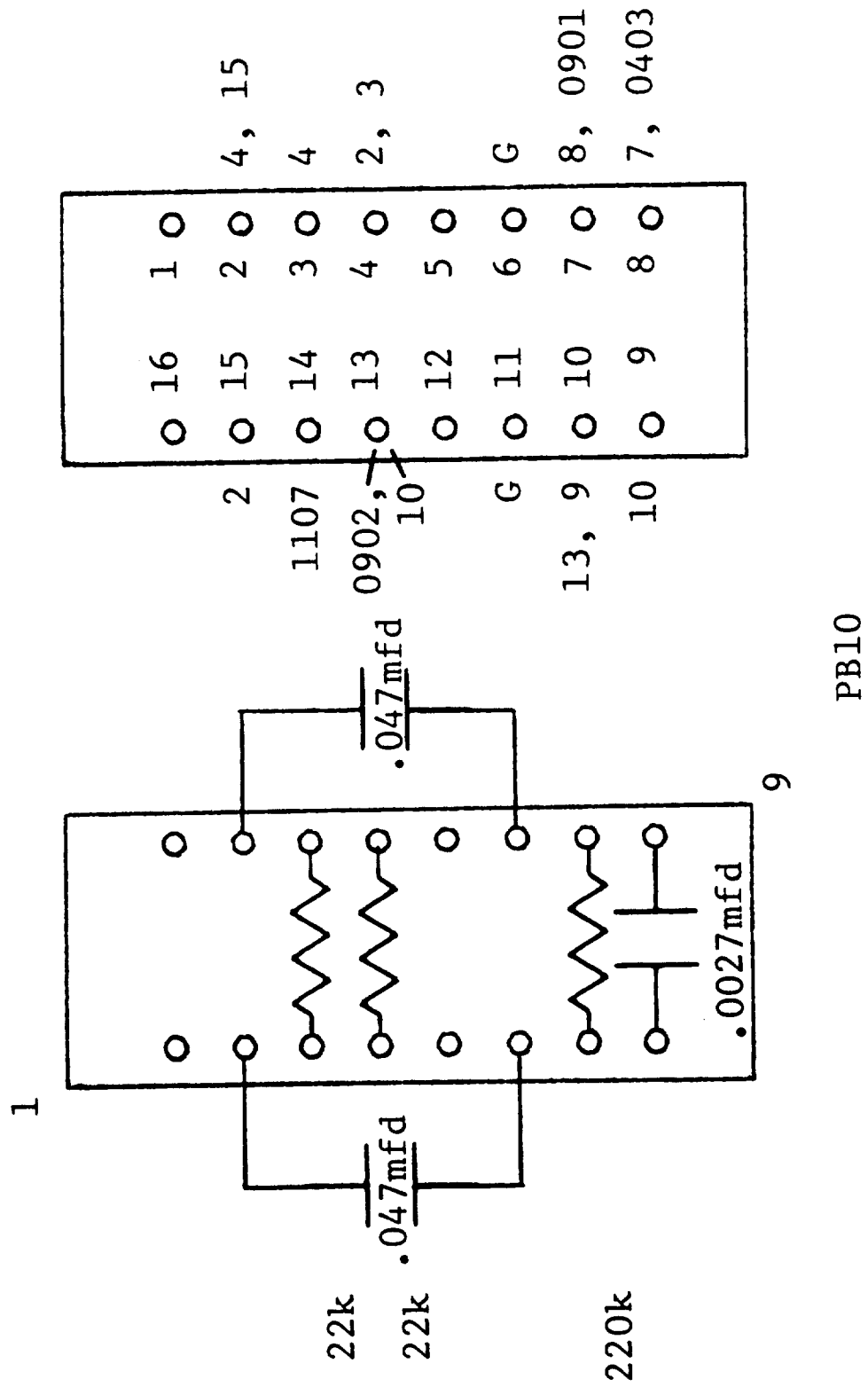
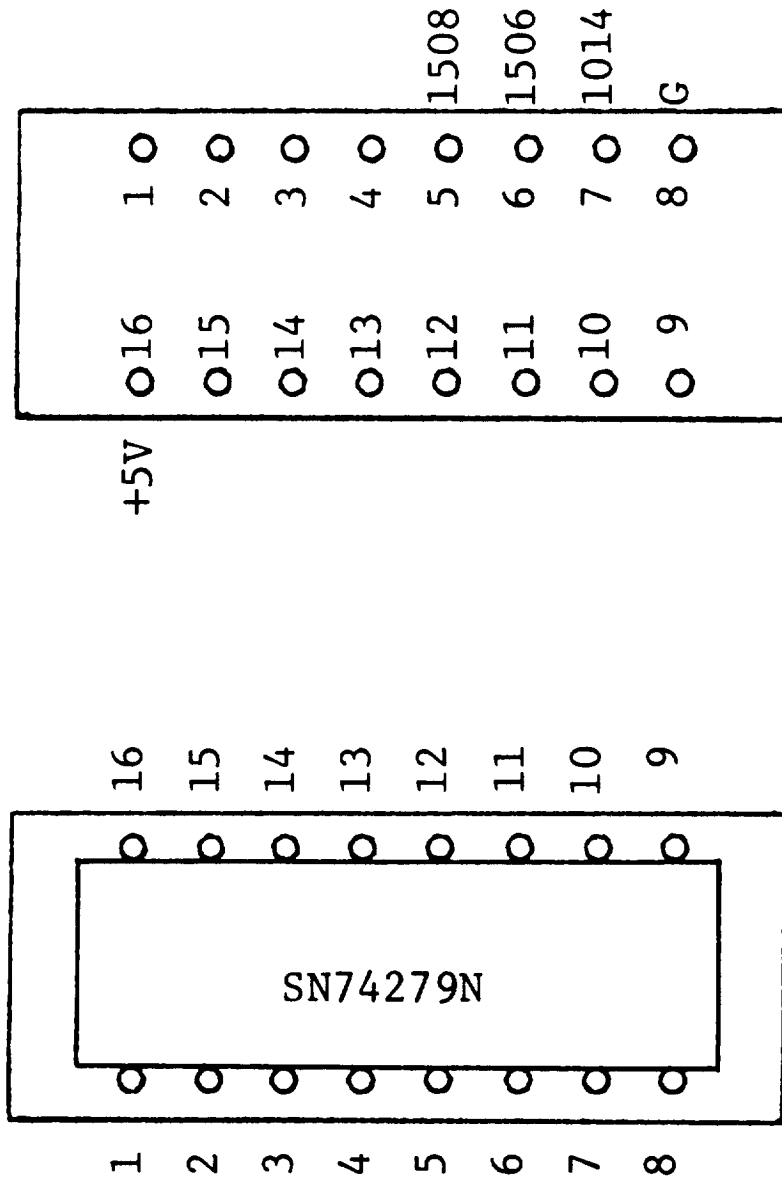
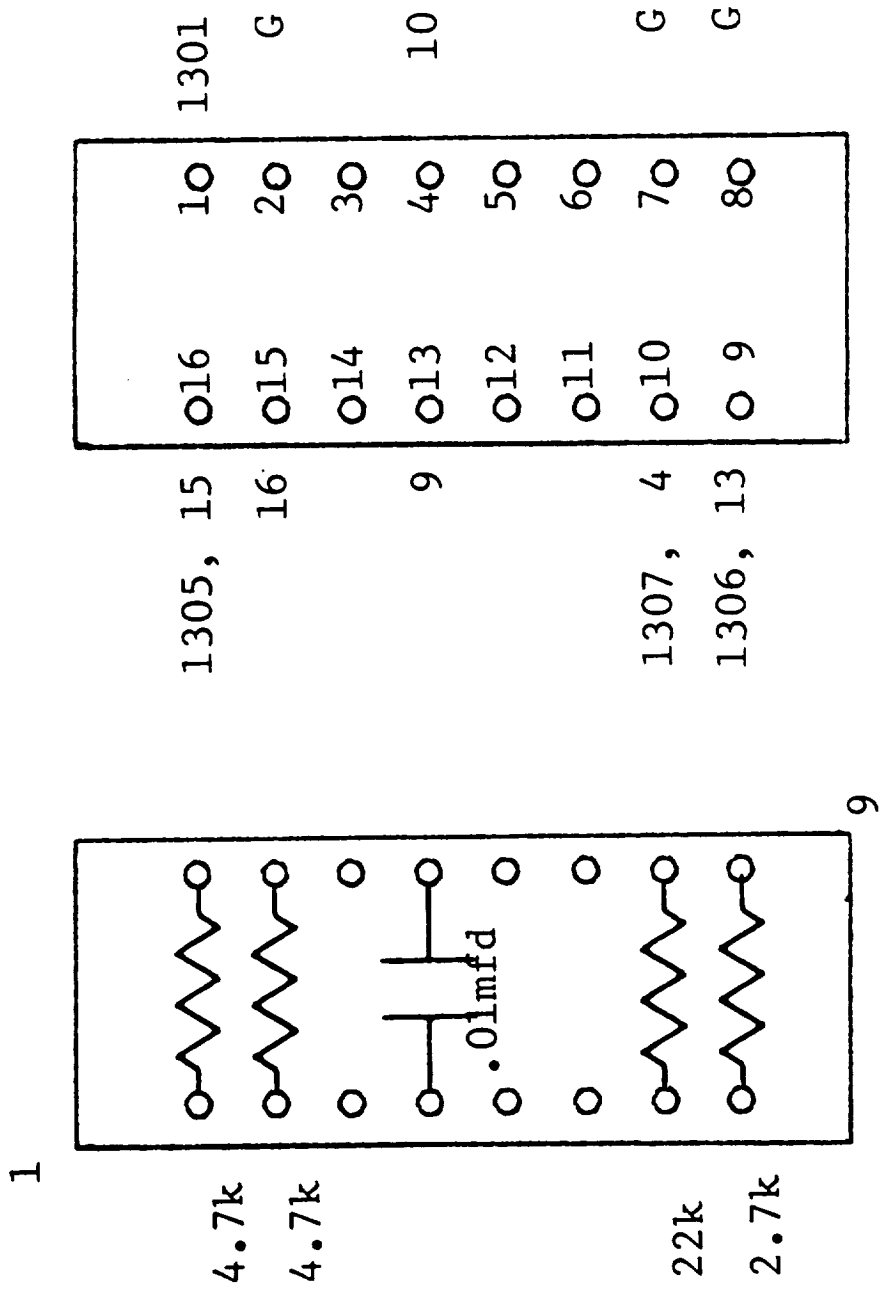


Figure 2.15. Wiring diagram with interconnections.



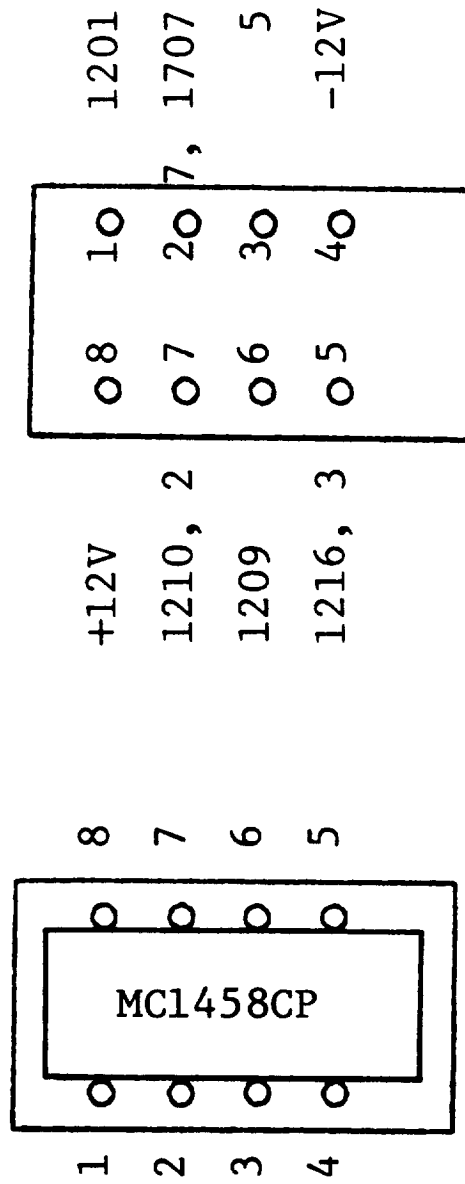
PB11

Figure 2.16. Wiring diagram with interconnections.



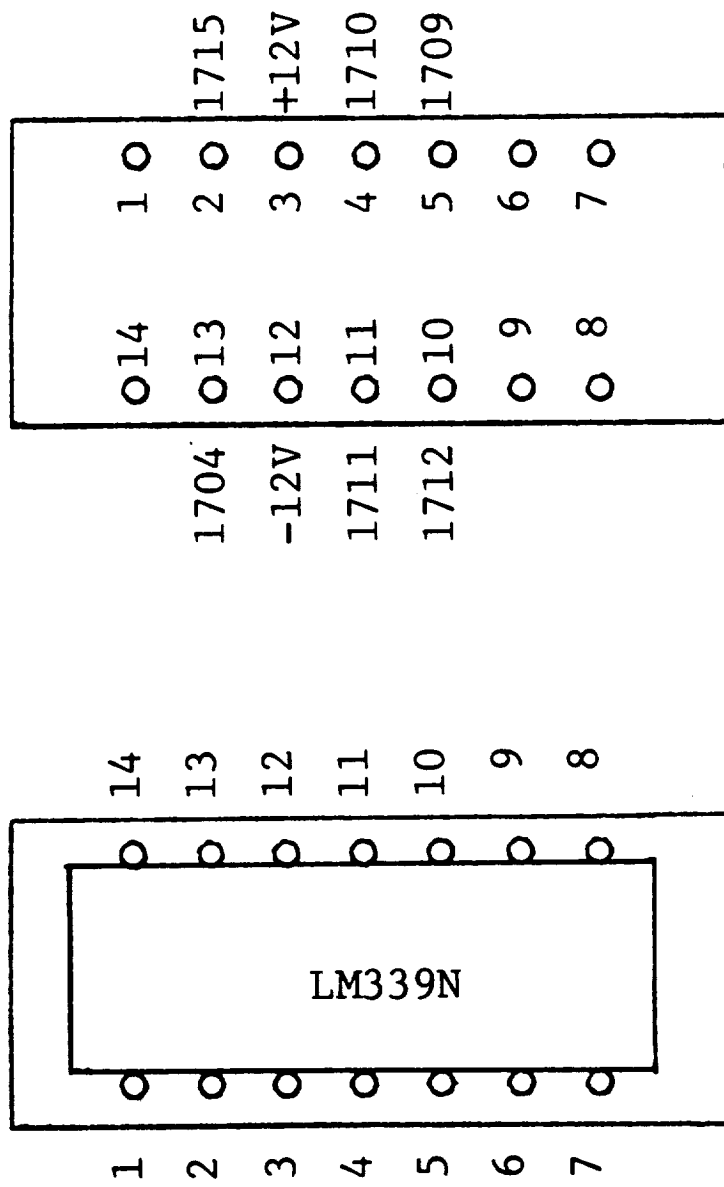
PB12

Figure 2.17. Wiring diagram with interconnections.



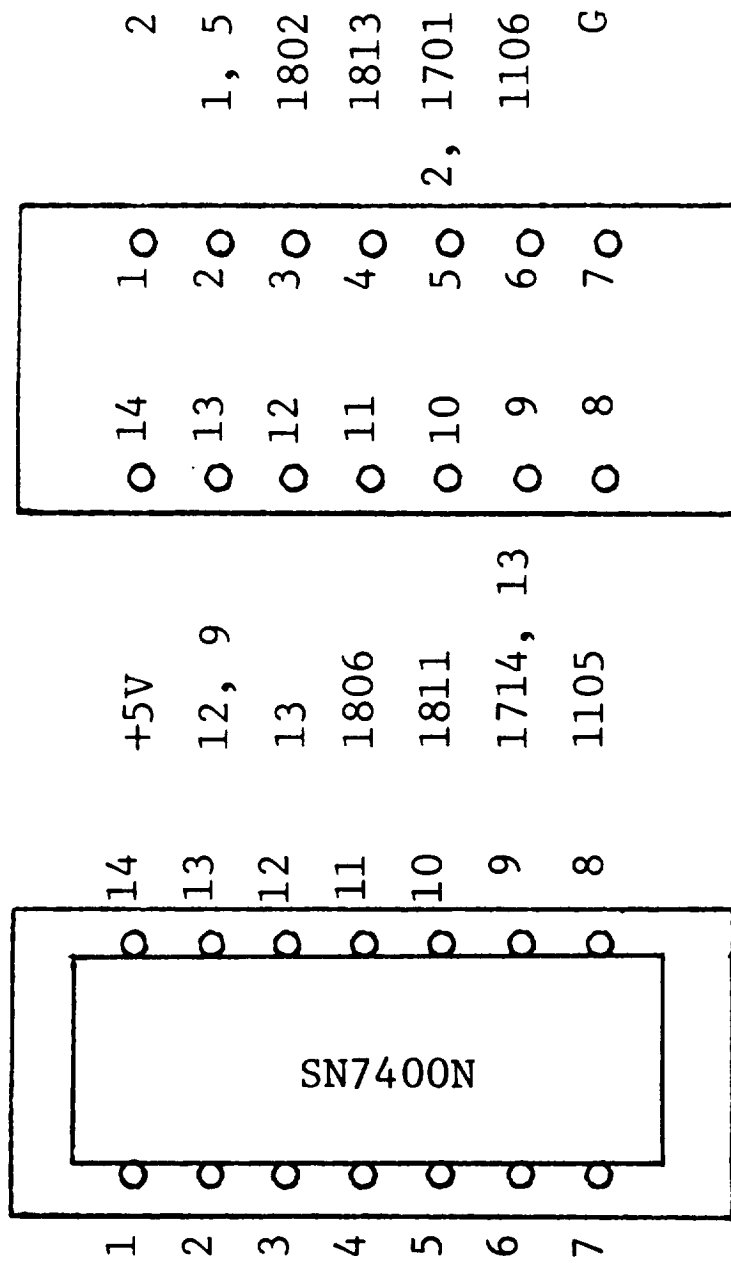
PB13

Figure 2.18. Wiring diagram with interconnections.



PB14

Figure 2.19. Wiring diagram with interconnections.



PB15

Figure 2.20. Wiring diagram with interconnections.

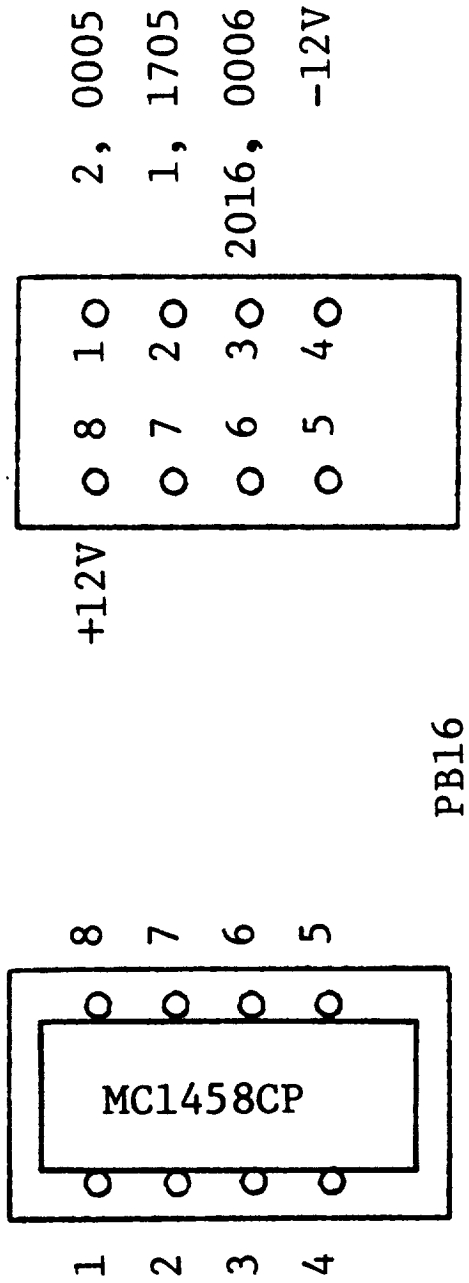
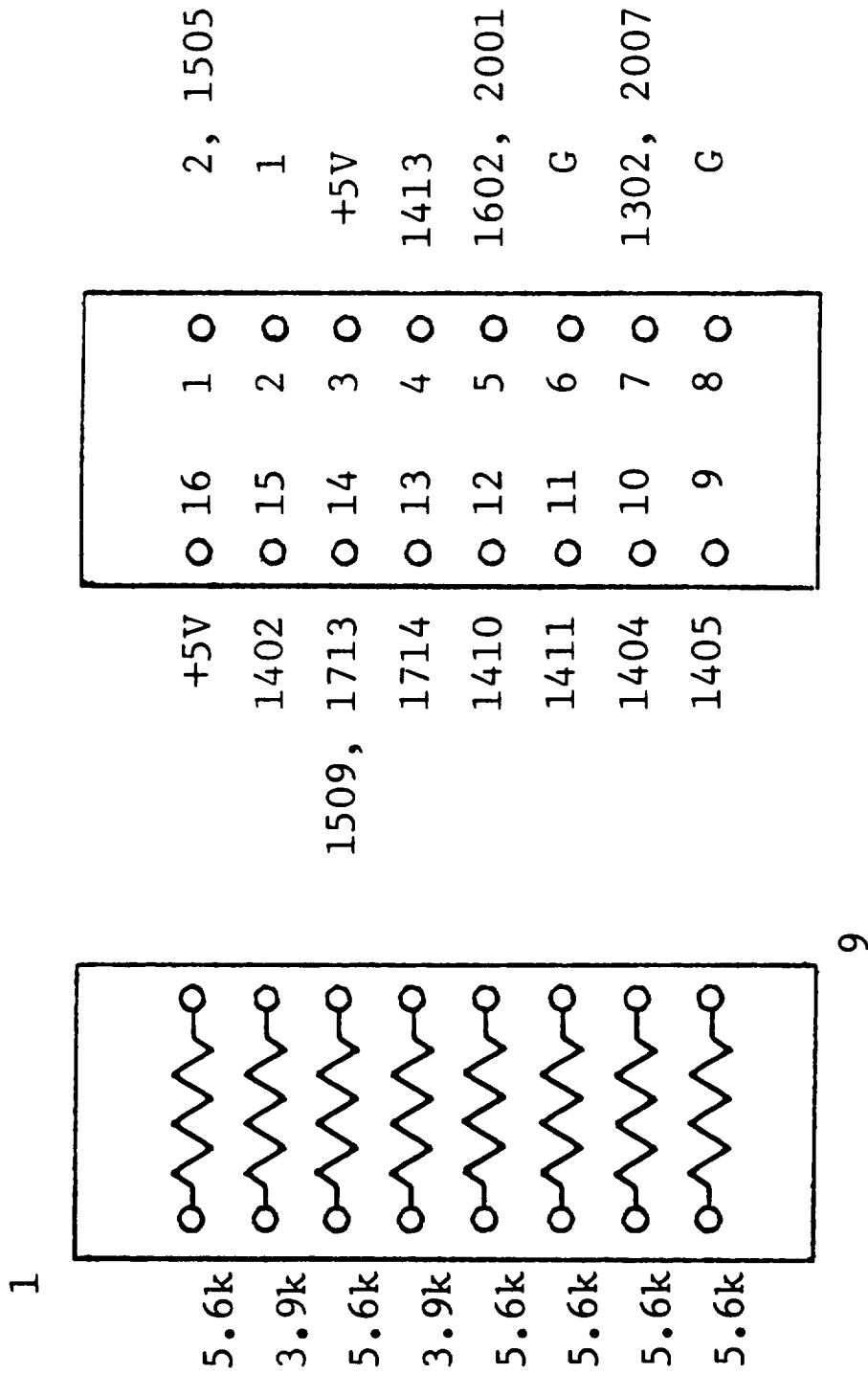
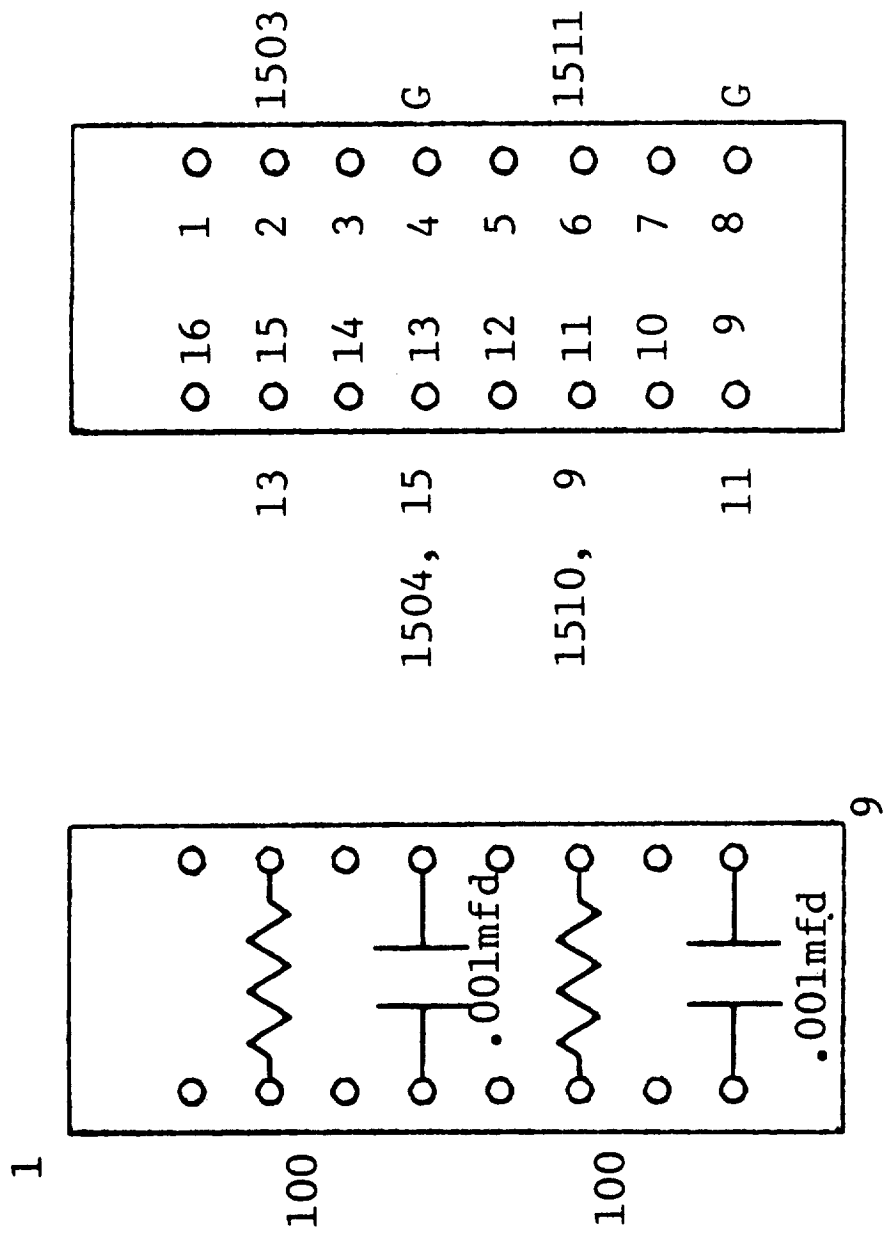


Figure 2.21. Wiring diagram with interconnections.



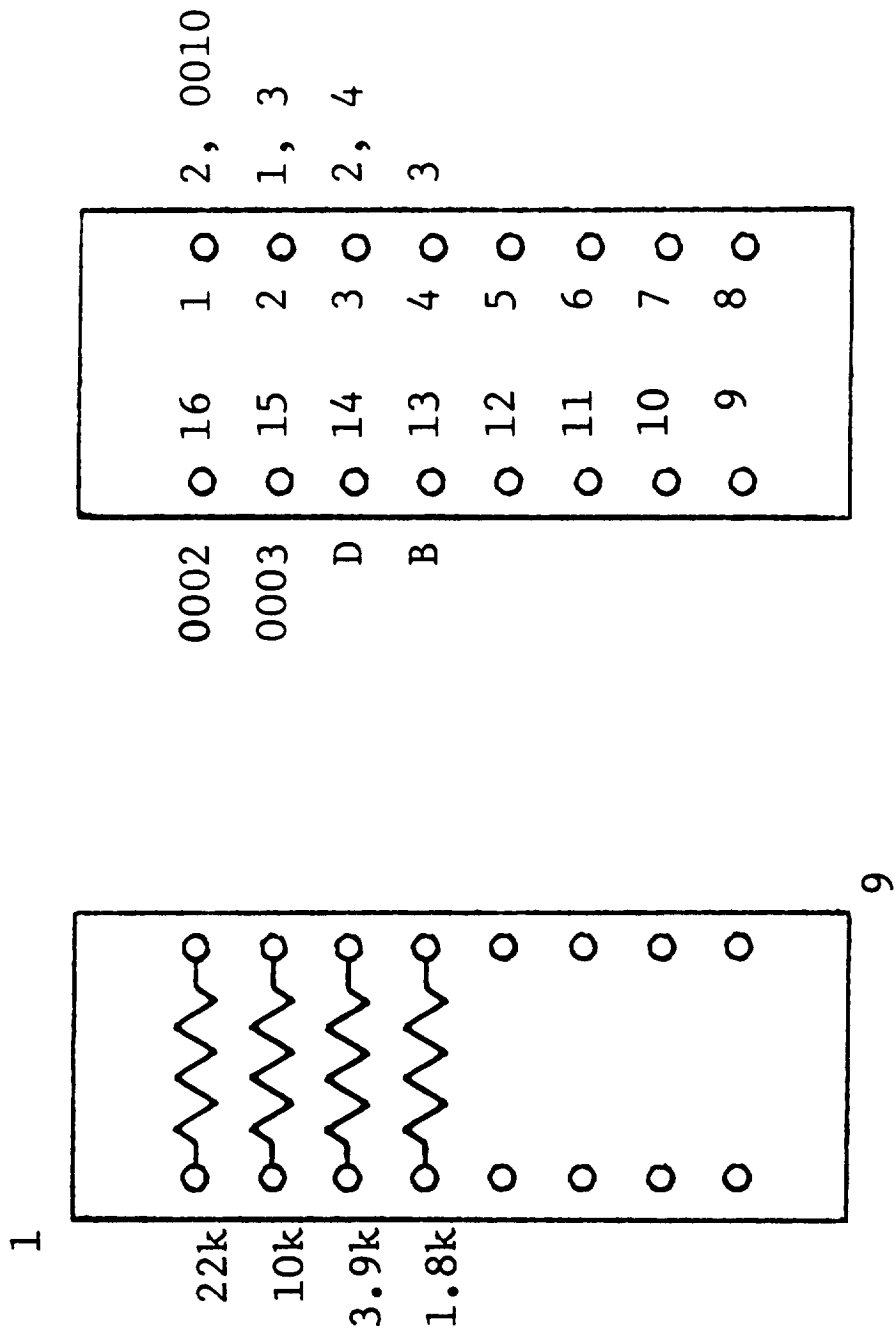
PB17

Figure 2.22. Wiring diagram with interconnections.



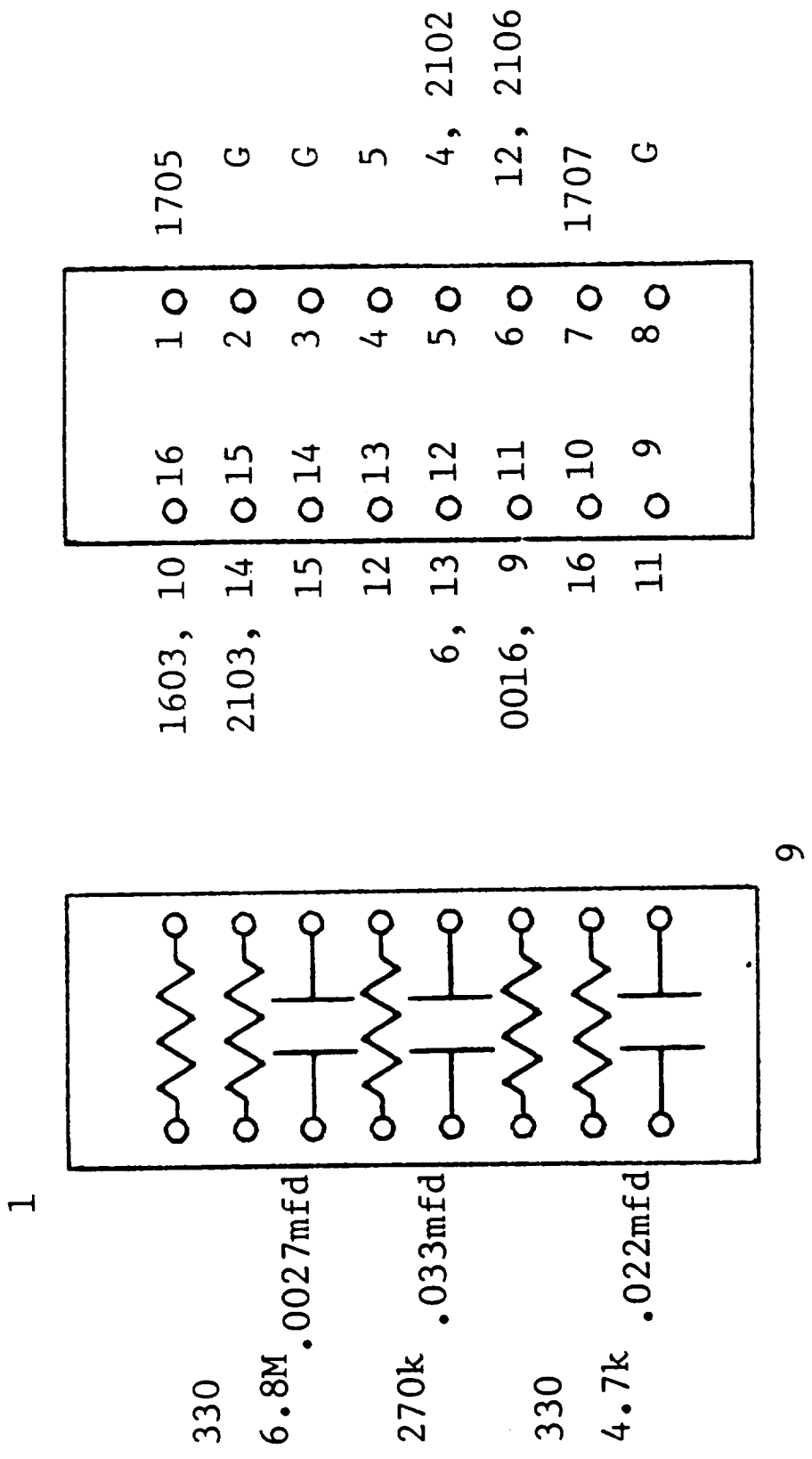
PB18

Figure 2.23. Wiring diagram with interconnections.



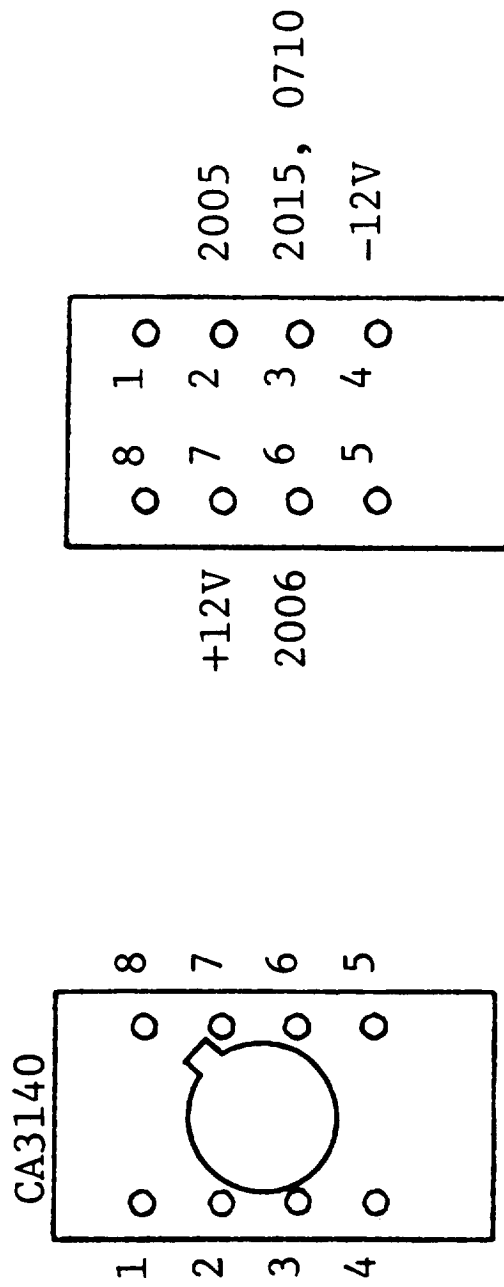
PB19

Figure 2.24. Wiring diagram with interconnections.



PB20

Figure 2.25. Wiring diagram with interconnections.



PB21

Figure 2.26. Wiring diagram with interconnections.

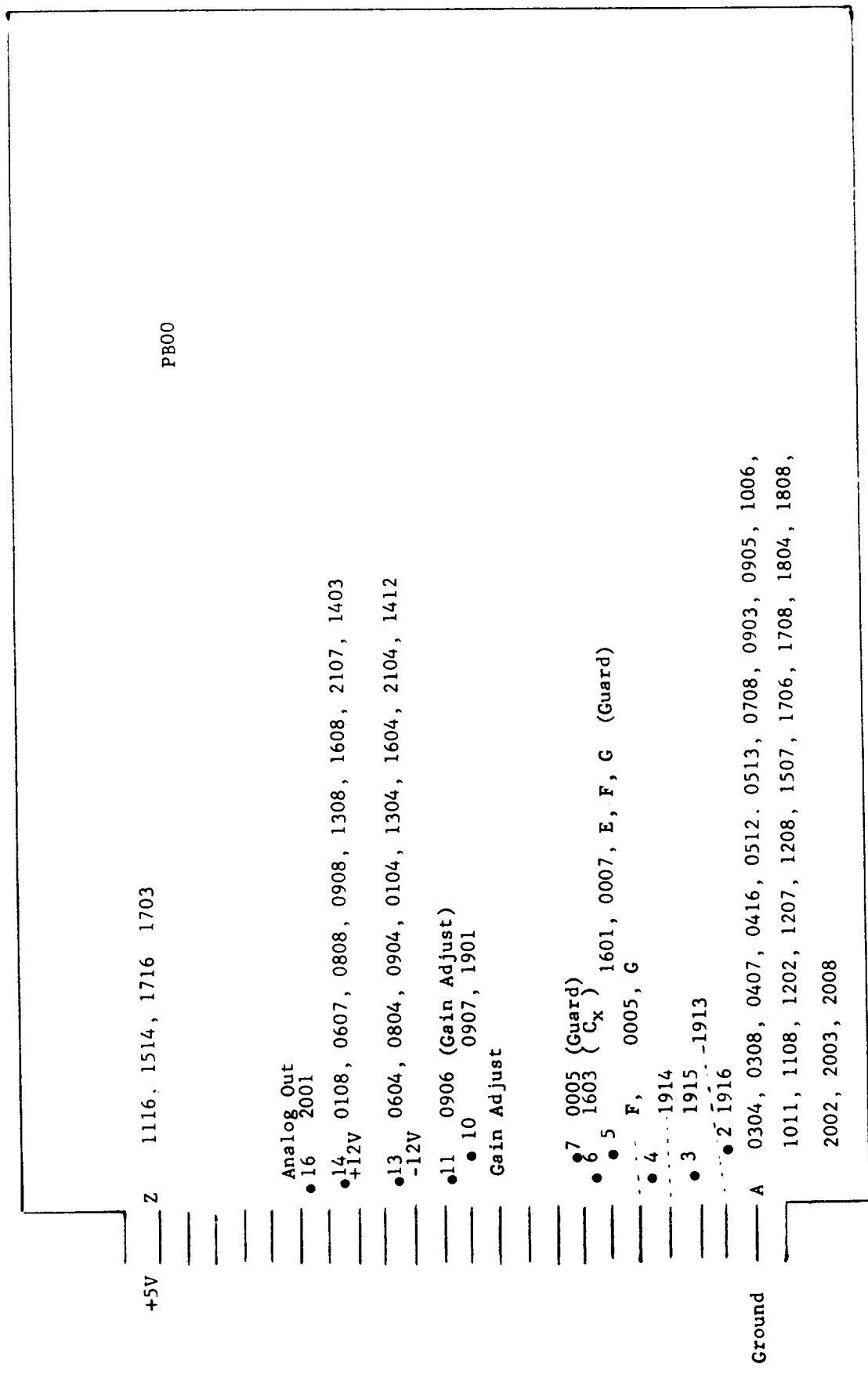


Figure 2.27. Plug-in tab connections.

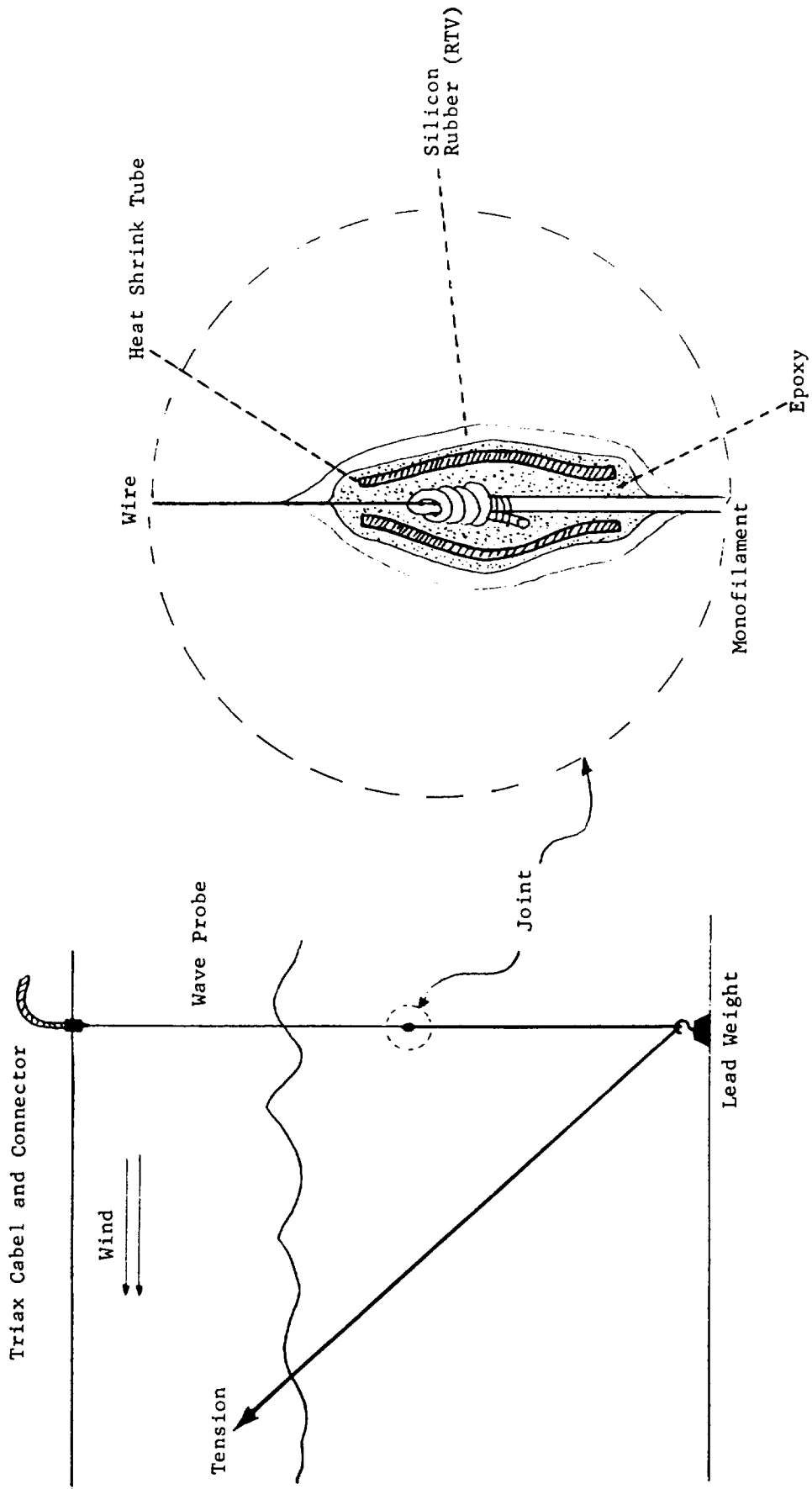


Figure 3.1. Laboratory arrangement of the wire probe.

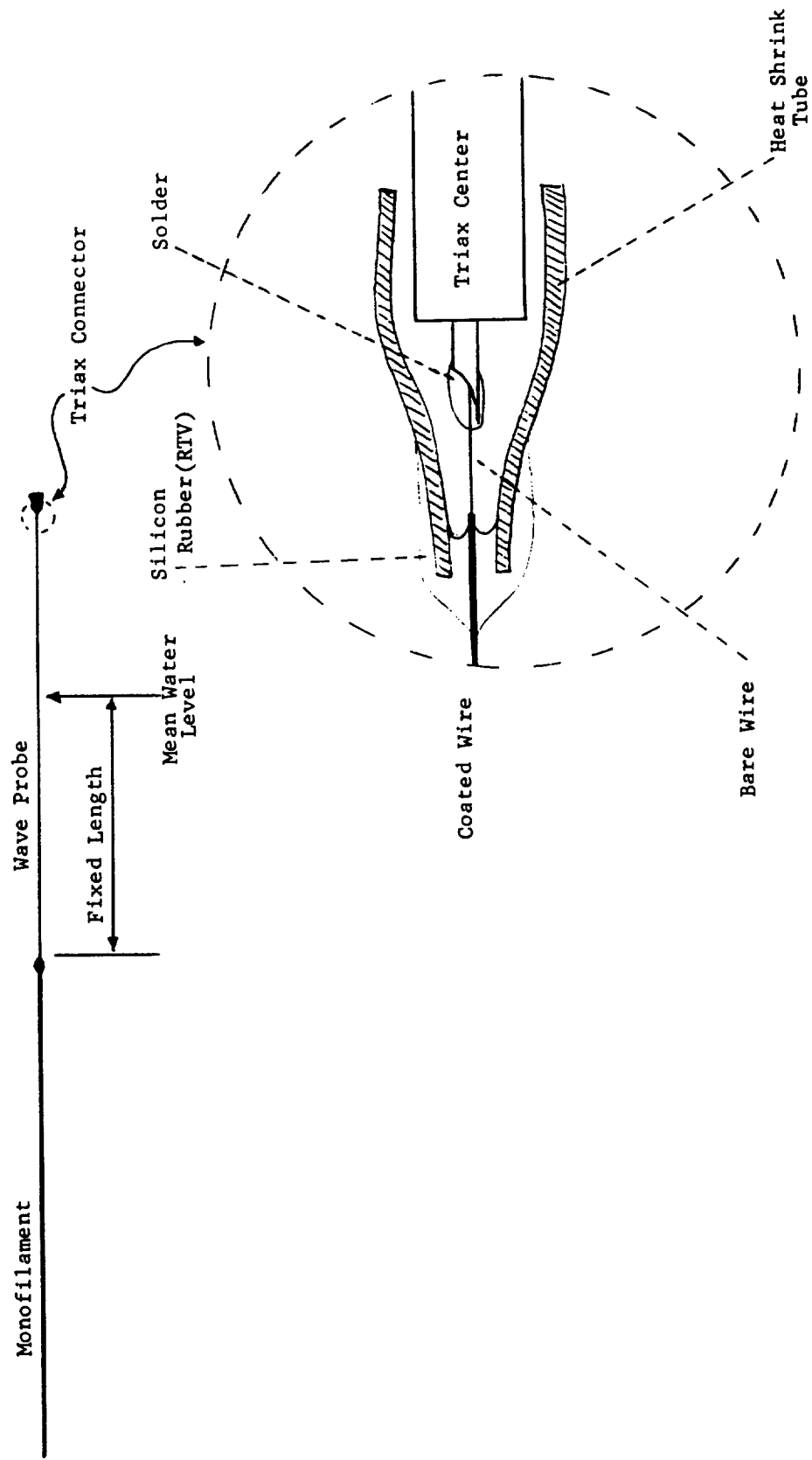


Figure 3.2. The triax connection.

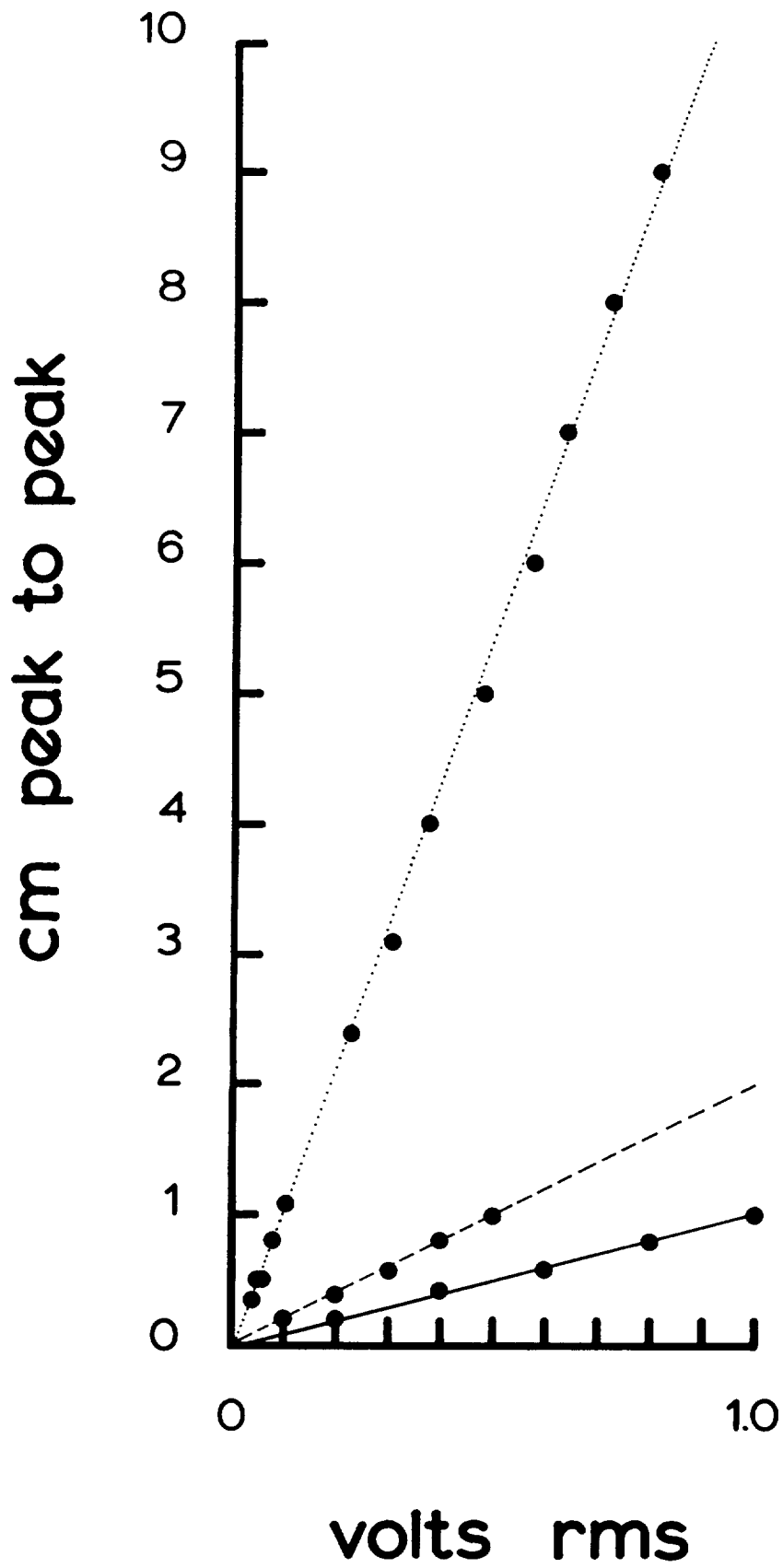


Figure 5.1. Typical results of probe calibration.

REPORT DOCUMENTATION PAGE			Form Approved OMB No. 0704-0188	
Public reporting burden for this collection of information is estimated to average 1 hour per response, including the time for reviewing instructions, searching existing data sources, gathering and maintaining the data needed, and completing and reviewing the collection of information. Send comments regarding this burden estimate or any other aspect of this collection of information, including suggestions for reducing this burden, to Washington Headquarters Services, Directorate for Information Operations and Reports, 1215 Jefferson Davis Highway, Suite 1204, Arlington, VA 22202-4302, and to the Office of Management and Budget, Paperwork Reduction Project (0704-0188), Washington, DC 20503.				
1. AGENCY USE ONLY (Leave blank)	2. REPORT DATE June 1992	3. REPORT TYPE AND DATES COVERED Reference Publication		
4. TITLE AND SUBTITLE A Self-Zeroing Capacitance Probe for Water Wave Measurements			5. FUNDING NUMBERS 970	
6. AUTHOR(S) Steven R. Long				
7. PERFORMING ORGANIZATION NAME(S) AND ADDRESS(ES) NASA Wallops Flight Facility Wallops Island Virginia 23337			8. PERFORMING ORGANIZATION REPORT NUMBER 92B00058	
9. SPONSORING/MONITORING AGENCY NAME(S) AND ADDRESS(ES) National Aeronautics and Space Administration Washington, D.C. 20546-0001			10. SPONSORING/MONITORING AGENCY REPORT NUMBER NASA RP-1278	
11. SUPPLEMENTARY NOTES Steven R. Long, Code 972, NASA WFF, Wallops Island, Virginia 23337.				
12a. DISTRIBUTION/AVAILABILITY STATEMENT Unclassified - Unlimited Subject Category 48			12b. DISTRIBUTION CODE	
13. ABSTRACT (Maximum 200 words) The wave probe developed at the Air-Sea Interaction Research Facility was designed to measure the surface elevation fluctuations of water waves. Design criteria included being linear in response, self-zeroing to the mean water level, having multiple operating ranges so that the instrument's maximum output could be matched to the maximum surface elevation over varying conditions, and be as noise-free as possible. The purpose of this publication is to provide a detailed description of the design and construction of this probe.				
14. SUBJECT TERMS Capacitance Probe, Water Waves, Ocean Surface Microscale			15. NUMBER OF PAGES 52	
			16. PRICE CODE A04	
17. SECURITY CLASSIFICATION OF REPORT Unclassified	18. SECURITY CLASSIFICATION OF THIS PAGE Unclassified	19. SECURITY CLASSIFICATION OF ABSTRACT Unclassified	20. LIMITATION OF AB- STRACT	